Award Number: W81XWH-14-1-0224

TITLE: Environmental Mycobiome Modifiers of Inflammation and Fibrosis in Systemic Sclerosis

PRINCIPAL INVESTIGATOR: Michael L. Whitfield, Ph.D

CONTRACTING ORGANIZATION: The Trustees of Dartmouth College
Hanover, NH 03755

REPORT DATE: September 2016

TYPE OF REPORT: Annual

PREPARED FOR: U.S. Army Medical Research and Materiel Command
Fort Detrick, Maryland 21702-5012

REPORT DOCUMENTATION PAGE	Form Approved OMB No. 0704-0188

1. REPORT DATE	2. REPORT TYPE	3. DATES COVERED
September 2016	Annual	20 Aug 2015 - 19 Aug 2016

4. TITLE AND SUBTITLE

Environmental Mycobiome Modifiers of Inflammation and Fibrosis in Systemic Sclerosis

5a. CONTRACT NUMBER

5b. GRANT NUMBER
W81XWH-14-1-0224

5c. PROGRAM ELEMENT NUMBER

6. AUTHOR(S)
Michael Whitfield, Ph.D, Patricia A. Pioli, Ph.D
Robert Lafyatis, MD
Sarah Arron, MD/Ph.D
E-Mail: Michael.L.Whitfield@dartmouth.edu

5d. PROJECT NUMBER

5e. TASK NUMBER

5f. WORK UNIT NUMBER

7. PERFORMING ORGANIZATION NAME(S) AND ADDRESS(ES)
The Trustees of Dartmouth College
Hanover, NH 03755

8. PERFORMING ORGANIZATION REPORT

9. SPONSORING / MONITORING AGENCY NAME(S) AND ADDRESS(ES)
U.S. Army Medical Research and Materiel Command
Fort Detrick, Maryland 21702-5012

10. SPONSOR/MONITOR'S ACRONYM(S)

11. SPONSOR/MONITOR'S REPORT NUMBER(S)

12. DISTRIBUTION / AVAILABILITY STATEMENT
Approved for Public Release; Distribution Unlimited

13. SUPPLEMENTARY NOTES

14. ABSTRACT

This project is focused on Systemic Sclerosis (SSc), a progressive fibrotic disease characterized by skin fibrosis and damage to internal organs. While a wide range of environmental and biological triggers have been proposed, no definitive etiologic agents have yet been identified. Metagenomic analysis of non-human sequences in SSc RNA-seq data was used to detect microbial sequences in human tissues in an unbiased, quantitative manner. Our studies suggest that disease pathogenesis includes a common environmental fungal trigger, *Rhodotorula glutinis*, which we hypothesize elicits immune activation in a permissive host genetic background.

Skin biopsies have been collected from SSc patients and analyzed by high-throughput sequencing, providing substantial gene expression data as well as detailed information regarding the host microbiome. Data have been compared against that of healthy control samples.

15. SUBJECT TERMS: IMSA, systemic sclerosis, scleroderma, mycobiome, fibrosis, gene, genetics, RNA-seq, *R. glutinis*, Metagenomics					
16. SECURITY CLASSIFICATION OF:			**17. LIMITATION OF**	**18. # OF PAGES**	**19a. NAME OF RESPONSIBLE PERSON** USAMRMC
a. REPORT U	**b. ABSTRACT** U	**c. THIS PAGE** U	UU	33	**19b. TELEPHONE NUMBER** *(include area code)*

Table of Contents

1. INTRODUCTION

Systemic sclerosis (SSc) is a heterogeneous disease of fibrosis and inflammation, concomitant with significant autoimmunity. SSc often presents with skin manifestations and Raynaud's phenomenon; the extent and location of fibrotic lesions in people with SSc contributes to the diagnoses of disease subtypes and prognosis. My laboratory has pioneered the use of gene expression subsets in SSc [2-6]. Most recently we have demonstrated enrichment of a mycobiome component (Rhodotorula glutinis) in SSc patient skin [7].

We describe our studies from the first year of the grant below. This work was accomplished by researchers at Geisel School of Medicine at Dartmouth, Boston University Medical Center and University of California, San Francisco under the partnering PI option.

2. KEYWORDS:

IMSA, systemic sclerosis, scleroderma, SSc, mycobiome, microbiome, fibrosis, gene, genetics, RNA-seq, Next Generation Sequencing, skin, *R. glutinis*, *Rhodotorula,* Metagenomics

3. ACCOMPLISHMENTS

Milestones were assigned to this proposal, with tasks to be accomplished by each investigator. The overall **summary** of our progress relative to these tasks is given below, followed by a complete discussion of our work this past year.

Milestone 1 Determine the identity and distribution of microbiome components across SSc skin**.**

Task 1 (Months 1-36) Whitfield Laboratory to perform RNA-seq analysis of SSc skin biopsies.

Including technical replicates, RNA-seq has been run on 22 SSc patient skin biopsies and 6 healthy controls to date; an additional 8 SSc patient biopsies are currently being processed. Recruitment of additional SSc patients and healthy controls is ongoing.

Task 2 (Months 6-36) Whitfield Laboratory to perform RNA-seq analysis for differentially expressed mRNAs and non-coding RNAs.

Raw sequence reads have been analyzed using publicly available software packages that have been optimized and validated by us.

Task 3 (Months 6-36) Arron group to perform IMSA and determine the identity of microbiome components.

Dr. Arron's group is currently performing metagenomic analysis on 28 new and existing skin biopsy samples (22 SSc and 6 healthy controls) from the Whitfield Laboratory.

Task 4 (Months 1-24) Arron group to create scaffolds from aligned reads for each microbiome component and develop nested PCR followed by targeted multiplexed sequencing assays for cost-effective screening.

We developed a fast and efficient nested PCR reaction targeting microbiome components specific for fungal species identification. We then evaluated the identity and number of fungal reads by next generation sequencing (see Task 5). We have found the data from this targeted mycobiome method to be lower quality than our metagenomic RNA-seq analyses and we are exploring targeted microbiome methods.

Our preliminary findings suggest significant bacterial dysbiosis in affected skin, with only modest changes in fungal abundance. Validation of these findings will therefore be run using targeted 16S sequencing to identify changes in bacterial composition. DNA has been collected for 116 skin samples (SSc and healthy controls) to date, with an additional 178 samples awaiting DNA purification. Targeted sequencing of the V2-4-8 and V3-6,7-9 hypervariable regions of 16S rRNA from these samples will be performed using the Ion 16S Metagenomics Kit (ThermoFisher), and sequenced on the Ion Torrent.

The original goal of this task was validation. Therefore, validation will also be performed by analyzing RNA-seq data generated as part of other studies (n > 100). This approach enables direct assessment of all microbiome components associated with affected skin, including archaea, bacteria, viruses, fungi, and parasites, as well as comparisons between microbiome composition and gene expression of associated tissues using the same computational methods.

Task 5 (Months 1-12) Whitfield Laboratory to examine a larger population of archived skin biopsy RNA to determine the prevalence of microbiome components across the SSc population.

See above.

Task 6 (Months 1-24) Culture microbiome components from the skin of SSc patients. Use of skin biopsies as a method for fungal culture was not successful.

Disappointingly, swabbing of affected skin of SSc patients has yet to result in recovery of clinically relevant fungi or other organisms. Swabbing and other culture-based methods of microbial detection will be revisited following completion of our RNA-seq analyses, enabling targeted isolation of organisms associated with SSc lesional skin.

Milestone 2 Identify the inflammatory infiltrates in SSc skin and their response to microbiome components

Task 1 (Months 1-6) Whitfield Laboratory to perform computational analysis/prediction of inflammatory cell infiltrates from whole genome expression data.

We used single sample Gene Set Enrichment Analysis (ssGSEA) to identify the cellular subsets in SSc skin at different stages of disease.

Task 2 (Months 6-24) Perform immunohistochemistry to validate the computational predictions of task 1.

We have optimized markers for different cell types in SSc skin. We have used CD163 for macrophages, CD1c for myeloid dendritic cells (mDCs), and CD3 for T cells in a separate study. Current work focuses on the identification of T cell subsets (CD4 and CD8), and B cells (CD19 and CD20). We can now use these markers to look at innate and adaptive immune cells in the patients of this study.

Task 3 (Months 1-18) Whitfield Laboratory to develop protocols for the isolation and characterization of immune cells from skin using the sclerodermatous Graft-Versus Host Disease (sclGVHD) mouse including detailed characterization of cell types.

We established the sclGVHD model in the laboratory. We have performed initial cell isolations and phenotyping of these samples.

Task 4 (Months 6-18) Identify the secreted mediators of fibrosis / inflammation being produced (Whitfield / Pioli). Once cells are isolated, we will screen for secreted pro-fibrotic mediators.

We have analyzed profibrotic mediators in these cells, work is ongoing.

Task 5 (Months 12-36) Apply protocols to characterize the inflammatory infiltrate in the skin of SSc patients (Whitfield / Pioli). After cell isolation procedures have been optimized in the sclGVHD mouse, we will examine the infiltrate and profibrotic mediators in SSc skin biopsies.

Protocols for isolating these cells from mouse skin have been optimized. Work is underway for human skin.

Milestone 3 Determine if SSc patients have a specific immune response against *R. glutinis* that is different from healthy controls and if this response can drive fibrosis.

Task 1 (Months 1-24) Test patient sera for cross-reactivity against *R. glutinis* antigens (Whitfield/Lafyatis).

We have performed western blots using whole cell lysates and probed with sera collected from both healthy controls and SSc patients.

Task 2 (Months 1-24) Identify the cross-reacting proteins by mass spectrometry (Whitfield).

Serum-immunoprecipitation of R. glutinis and human HeLa cell whole cell lysates followed by mass spectrometry was performed to identify immunoreactive proteins associated with R. glutinis. We have written a manuscript on the human cross-reactivity. We are having difficulty with the annotation state of the R. glutinis genome for annotating those spectra.

Task 3 (Months 12-36) Use isolated PBMCs and isolated monocytes to examine the cytokines secreted and changes in gene expression when cells are exposed to *R. glutinis* or other putative micro / mycobiome triggers (Whitfield/Pioli).

Work underway.

Task 4 (Months 12-24) Determine if chronic exposure to *R. glutinis* or other micro / mycobiome components stimulate a fibrotic response in a mouse model of SSc. (Whitfield).

Work underway.

PRELIMINARY RESULTS BY MILESTONE

Milestone 1: Determine the identity and distribution of microbiome components across SSc skin

Task 1: RNA-Seq analysis of SSc skin. Including technical replicates, RNA-seq has been run on 18 SSc patient skin biopsies to date. Recruitment of additional SSc patients and healthy controls is ongoing. mRNA from 22 SSc patients and 6 healthy controls have been sequenced, yielding 30-237 million paired-end reads per sample. Reads were then aligned to the human genome (hg19 assembly). Approximately 70%-80% of reads were uniquely mapped, which is in line with expectations (Table 1).

Table 1. Statistics of alignment

Sample ID	Disease Type	Total Reads	Uniquely Mapped	Mapped length	% multi-mapped	% Unmapped
MK01-FA	SSc	79642964	0.6	148	0.37	0.03
MK01-B	SSc	87465540	0.45	148	0.53	0.02
AM02-FA	SSc	82459754	0.7	148.1	0.28	0.02
AM02-B	SSc	89078313	0.64	148.1	0.34	0.02
KB03-FA	SSc	110881994	0.8	148.1	0.17	0.03
KB03-B	SSc	80684936	0.76	148	0.14	0.1
JP04-FA	SSc	86911206	0.73	148	0.15	0.12
JP04-B	SSc	87609067	0.54	148	0.36	0.1
KB05-FA	SSc	78252845	0.72	148	0.16	0.12
KB05-B	SSc	105842068	0.67	147.7	0.27	0.06
KL06-FA	SSc	103150299	0.81	148	0.15	0.04
KL06-B	SSc	75717290	0.64	148.2	0.34	0.02
SH07-FA	SSc	85776797	0.67	145.7	0.13	0.2
SH07-B	SSc	113066228	0.75	148	0.2	0.04
N01_Base	SSc	82992452	0.67	148	0.31	0.03
N05_Base	SSc	77151907	0.74	148.1	0.23	0.02
N07-Base	SSc	87025838	0.8	148.1	0.18	0.02
N09_Base	SSc	86468461	0.73	148.1	0.25	0.02
N10_Base	SSc	100362240	0.62	147.7	0.31	0.07
N11_Base	SSc	105056505	0.47	147.9	0.47	0.05
N15_Base	SSc	81209030	0.81	147.8	0.12	0.07
N18_Base	SSc	72275968	0.8	147.6	0.13	0.07
N13-2	Control	80255529	0.64	148.1	0.34	0.02
N15-3	Control	92668648	0.67	147.4	0.31	0.02
N15-5	Control	84968648	0.59	147.9	0.38	0.04
N15-15	Control	92222389	0.32	148	0.61	0.06
N15-21	Control	103634414	0.32	147.6	0.58	0.06
N15-24	Control	75379182	0.78	148	0.14	0.08

Task 2 RNA-seq analysis for differentially expressed mRNAs. In order to identify differentially expressed mRNA, we used RSEM software to estimate the abundance of each mRNA transcript. Each sample was normalized using quantile normalization. Batch biases generated by the inclusion of previously sequenced samples from a separate study (N_Base samples) was performed with ComBat (Figure 1).

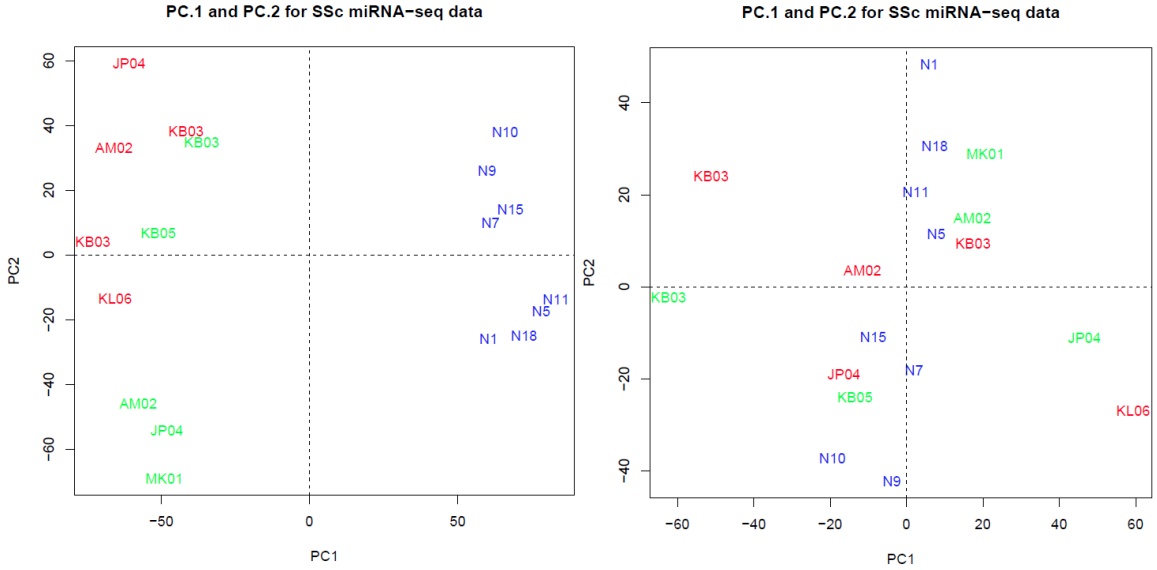

Figure 1. PCA plot of measurements. (Left) no ComBat correction; (Right) with ComBat correction.

As an initial analysis of these data, we chose to examine the consensus genes from Mahoney et al. [4]. These are genes that were consistently and reproducibly associated with individual SSc intrinsic gene expression subsets across three independent patient cohorts. Expression of these genes in our RNA-seq data reveals increased expression in the inflammatory and fibroproliferative subsets of patients (Figure 2). Expression of these genes is shown both before and after batch correction. Intermixing of samples is clearly evident after ComBat correction, indicating that batch correction was successful.

Figure 2. Heatmap of Mahoney_267modules. (Left) no ComBat correction; (Right) with ComBat correction. The attached heatmap only shows the samples from year 1 as the current set of samples are undergoing analysis.

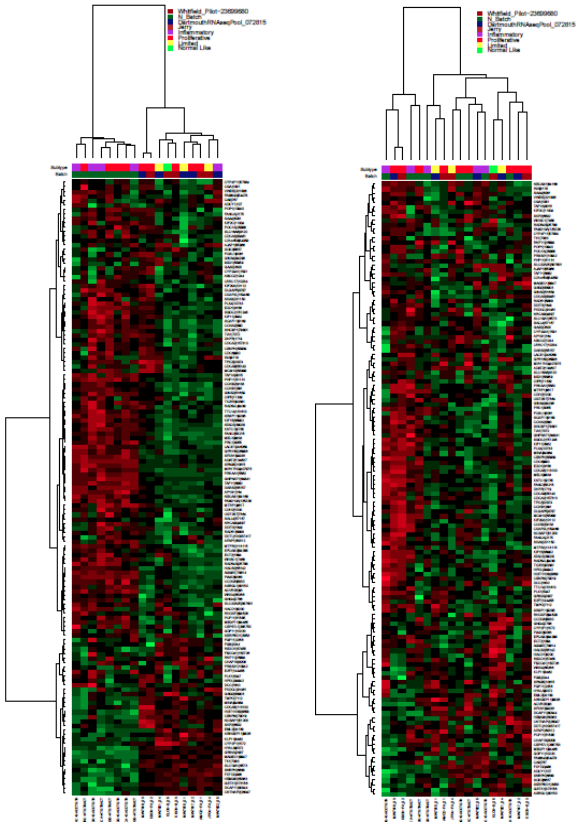

Task 3: IMSA analysis to identity microbiome components. In order to map the microbiome components present in these skin biopsies, IMSA has been performed on RNA-seq data from 28 skin biopsies (22 SSc and 6 healthy controls). We performed quality filtering and human sequence filtering using human genome (hg19). Over 99% of the total readset was derived from human or nonhuman primates in both SSc and control samples. IMSA was used to map reads to the NCBI non-redundant nucleotide (nt) database and generate taxonomy reports.

In preliminary data, we found that only inflammatory samples have high *Rhodotorula glutinis* target read counts (Figure 3), consistent with the preliminary data we presented in our initial grant proposal. Therefore, this preliminary analysis validates those original data.

Figure 3. IMSA analysis of RNA-seq data from SSc skin biopsies. SSc skin biopsies were divided by intrinsic gene expression subset, as previously described [3, 8]. Each biopsy was analyzed for *R. glutinis* sequences and IMSA score plotted for each subset.

We used a process called rarefaction to account for the variable read depth of different samples. We used using Quantitative Insights Into Microbial Ecology (QIIME) to perform rarefaction of outputs, a process by which taxa are randomly sampled without replacement; this process is necessary to ensure even sampling depth across patients. Alpha and beta diversity measures are calculated from these data.

Comparisons of SSc and controls revealed statistically significant differences in abundance between five of the top seven genera, with observed increases in SSc skin in the mRNA of major bacterial commensals such as *Propionibacterium*, *Staphylococcus*, and *Corynebacterium*; decreases were observed in *Citrobacter* and *Vibrio*, relative to controls ($p = 0.019$, $p = 0.004$, and $p = 0.002$, respectively; Figure 4A). *Rhodotorula* levels overall were not significantly different between SSc and controls in this cohort, which we believe is likely the result of differences in patient populations, with this second patient cohort consisting primarily of later disease duration. Biopsies from additional 8 untreated, early-stage SSc patients are being processed further validate the presence of *R. glutinis*.

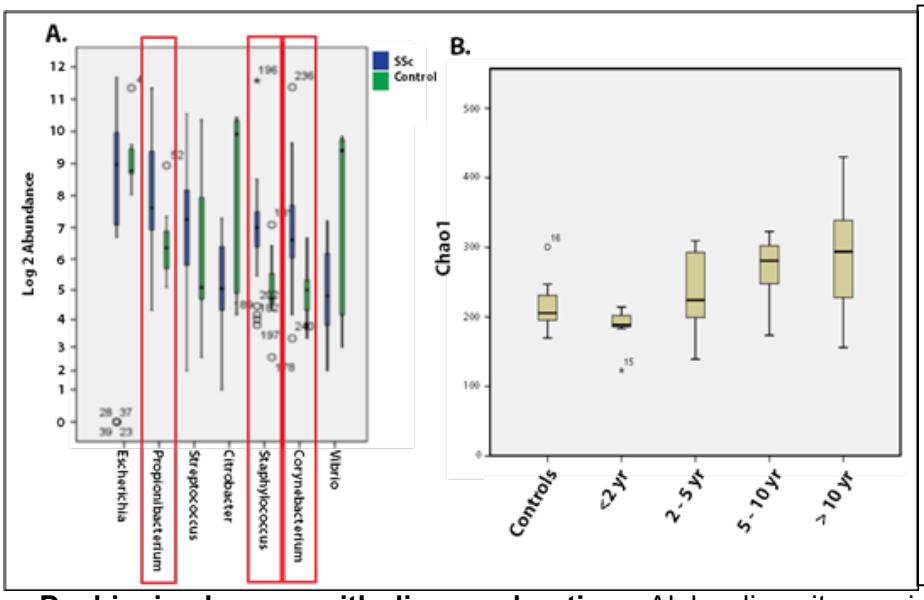

Figure 4. Differences in microbiome composition between SSc patients and controls. Significant differences in genus-level abundance and alpha diversity were observed between groups. A) Abundance of major genera in SSc (blue) vs controls (green); red boxes indicate organisms significantly more abundant in SSc. B) Alpha diversity analysis (Chao1) of SSc patients by disease duration. Samples were divided into 5 groups: controls, < 2 years, 2-5 years, 5-10 years, and > 10 years.

Dysbiosis changes with disease duration. Alpha diversity provides a measure of inter-sample diversity. Analysis of our SSc samples reveals significant changes in microbiome composition associated with disease duration (p = 0.011 by Chao1). Comparisons were performed using 4 disease duration groups, defined as < 2 years, 2-5 years, 5-10 years, and > 10 years, with or without healthy controls. Early stage patients (disease duration < 2 years after first non-Raynaud's symptoms) exhibit less microbiome diversity, followed by increasing diversity thereafter (Figure 4B). The most significant differences were observed between patients <6yr disease duration compared with those with >6yr (p = 0.001).

Linking microbiome dysbiosis to host gene expression changes. We examined our data for gene expression changes that were linked to differences in microbiome composition in each patient sample. Gene expression for each of the 28 skin biopsies was calculated from the RNA-seq data for the intrinsic genes from Johnson, *et al*. [1] (Figure 5). Hierarchical clustering of these data showed clear inflammatory (purple branches) and non-inflammatory (green branches) patients (Figure 5A). The inflammatory group shows high expression of genes associated with immune activation (Figure 5C). In these data, this split is significantly associated with disease duration, with early stage patients (red blocks; disease duration <5 years) clustering within the inflammatory group (Figure 5B). With one exception, all late stage patients (blue blocks; disease duration >5 years) and healthy controls (green blocks) clustered on the non-inflammatory branch (Figure 5B). The strong fatty acid and lipid metabolism signature evident in healthy controls, and a small number of inflammatory patients (Figure 5D), suggest multiple intrinsic subsets. Consistent with our data above, patients in the inflammatory group have low microbiome diversity (i.e. significant dysbiosis) while samples in the non-inflammatory group have increased microbiome diversity. **Therefore, there is a correlation between presence of the inflammatory gene expression signature and decreased microbiome diversity.**

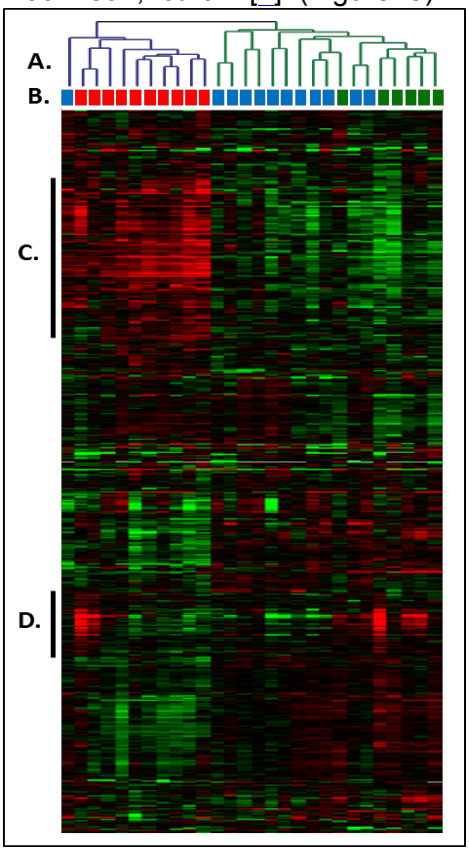

Figure 5. Gene expression may influence microbiome composition in skin. RNA-seq analysis of 28 skin biopsies (22 SSc and 6 controls) were median centered by gene and clustered using the intrinsic gene list described in Johnson et al [1] collapsed by unique gene, resulting in 1826 genes. **A)** Samples clustered into inflammatory (purple) and non-inflammatory groups based primarily on B) disease duration (red = < 5 years; blue = > 5 years; green = healthy controls). **C)** Inflammatory and **D)** lipid signaling gene expression modules are the strongest signals affecting clustering.

Based on these data, we find substantial differences between microbial populations of SSc skin with increasing disease duration. Within SSc patients, alpha diversity was significantly lower in the inflammatory group relative to non-inflammatory patients (p = 0.004 for Chao1), generally characterized by a small number of dominant genera, such as *Escherichia* and *Propionibacterium*. **These data suggest that changes in the cutaneous microbiome of SSc patients may directly contribute to immune activation in these patients.**

Tasks 4 and 5. Develop a nested PCR-based assay followed by targeted multiplexed sequencing as a cost-effective method for screening archived skin biopsy RNA to determine the prevalence of microbiome components across the SSc population. Improvements in our sample-processing pipeline now allow for simultaneous extraction of DNA, RNA, and miRNA from all patient biopsies. DNA is being used as a template for targeted sequencing of the intergenic transcribed spacer regions (ITS), a region widely regarded as the gold standard for fungal species identification. To date, targeted ITS sequencing libraries have been analyzed from 48 archived samples (39 SSc and 9 controls), which includes both paired lesional and non-lesional skin as well as multiple time points from a single patient (Figure 5). Sequencing outputs are being analyzed by IMSA to identify differences in microbial diversity and species abundance between patients and controls, between lesional and non-lesion skin, as well as how these populations change over time.

Our preliminary findings from our RNA-seq data suggest significant bacterial dysbiosis in affected skin, with only modest changes in fungal abundance. Validation of these findings will therefore be run using targeted 16S sequencing to identify changes in bacterial composition. DNA has been collected for 116 skin samples (SSc and healthy controls) to date, with an additional 178 samples awaiting DNA purification. Targeted sequencing of the V2-4-8 and V3-6,7-9 hypervariable regions of 16S rRNA from these samples will be performed using the Ion 16S Metagenomics Kit (ThermoFisher), and sequenced on the Ion Torrent.

Figure 6. Targeted ITS sequencing of normal and SSc skin biopsies. Below is a preliminary analysis of targeted fungal ITS sequencing which shows a subset of patients have increased *R. glutinis* sequences (red). The most prominent fungal species detected on skin were *Malassezia* spp. (blue), the most common genus of skin commensal fungi.

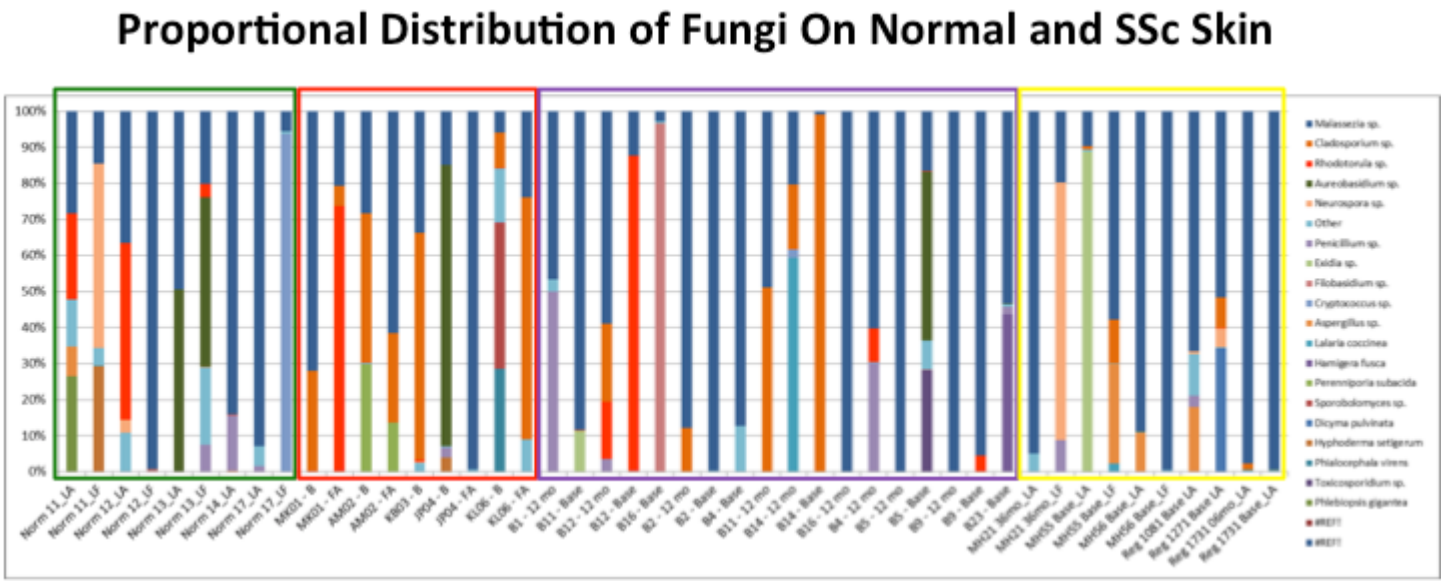

Task 6: Culture microbiome components from the skin of SSc patients. As mentioned above, *swabbing of affected skin of SSc patients has unfortunately yet to result in recovery of clinically relevant fungi or other organisms. Swabbing and other culture-based methods of microbial detection will be revisited following completion of our RNA-seq analyses, enabling targeted isolation of organisms associated with SSc lesional skin.* This may be due to the use of antiseptics prior to biopsy collection as a means of preventing infection of the biopsy site.

Milestone 2: Identify the inflammatory infiltrates in SSc skin and their response to microbiome components

Task 1: Computational prediction of inflammatory cell infiltrates from genomic expression data. We have used single sample Gene Set Enrichment Analysis (ssGSEA) to identify the cellular subsets in SSc skin at different stages of disease. We first benchmarked the ssGSEA method in my laboratory using publicly available gene expression data from pools of cell lines that had a known composition (data not shown). These

data demonstrated that ssGSEA accurately predicted cell type enrichment. We then analyzed a set of patients for whom we had whole genome expression data and that had strong expression of the inflammatory signature. We find the inflammatory signature is most strongly correlated with gene expression signatures from activated Dendritic Cells (DCs) and macrophages (MØs) (Figure 6). These methods are being applied in conjunction with the samples being analyzed in milestone 1.

Figure 7. Correlation of cell type signatures with a patient's inflammatory signature normalized enrichment score (NES). The inflammatory signature in SSc skin is most highly correlated with activated DCs and MØs.

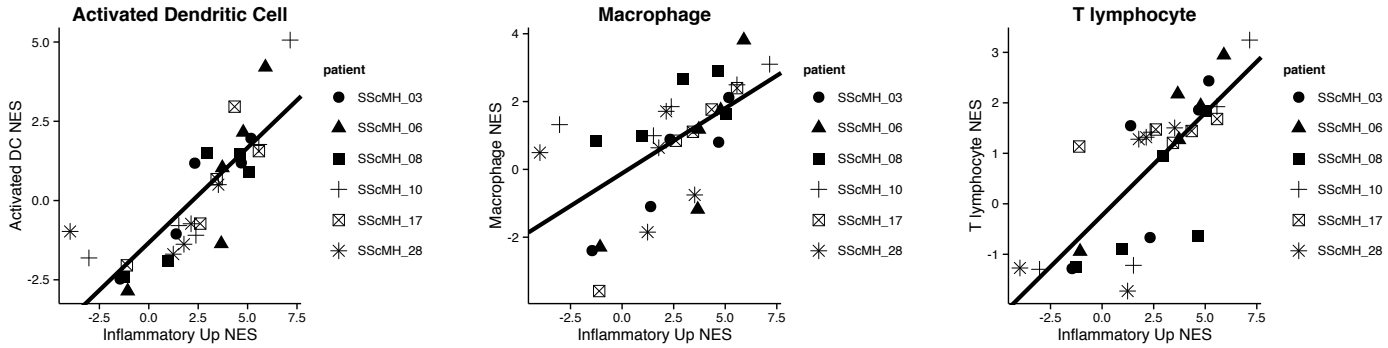

Task 2: Perform immunohistochemistry to validate the computational predictions of task 1 above. We have optimized markers for different cell types in SSc skin.

We have optimized markers for different cell types in SSc skin. We have used CD163 for macrophages, CD1c for myeloid dendritic cells (mDCs) and CD3 for T cells in a separate study. We can now use these markers to look at innate and adaptive immune cells in the patients of this study. We have optimized these stains in a set of SSc samples and will now be performing these stains in samples for this study. T cell subsets will be identified using antibodies against CD4 and CD8, and CD19 and CD20 will be used to determine B cell localization.

Task 3: Develop protocols for the isolation and characterization of immune cells from skin using the sclerodermatous Graft-Versus Host Disease (sclGVHD) mouse including detailed characterization of cell types.

We established the sclGVHD model in the laboratory and can recapitulate both skin thickening (Figure 8) and the aberrant gene expression profiles observed in our prior studies (Figure 9). We have performed initial cell isolations and phenotyping of these samples (Figure 10).

A. Allogeneic Transfer (sclGVHD) **B. Syngeneic Transfer (control)**

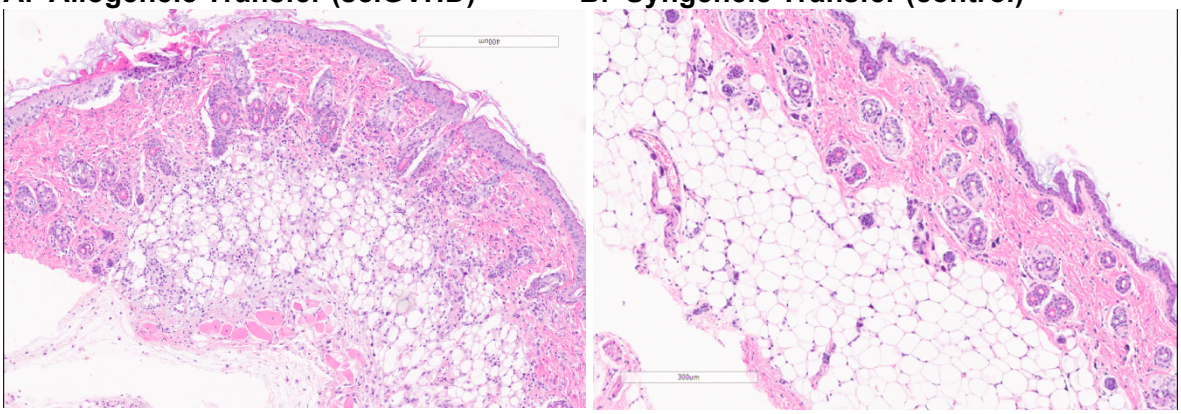

Figure 8. Immunohistochemistry was performed to show increased fibrosis at 2 weeks after disease intitiation. As expected we observe skin thickening in the sclGVHD mouse that is not observed in controls.

Gene expression analyses were performed on skin biopsies from the sclGVHD mouse and compared to our prior study of this model [9]. We find gene expression changes were produced and consistent with those observed when the model was generated at Harvard (Figure 9). Therefore, we can clearly reproduce this model faithfully, including the molecular SSc phenotype.

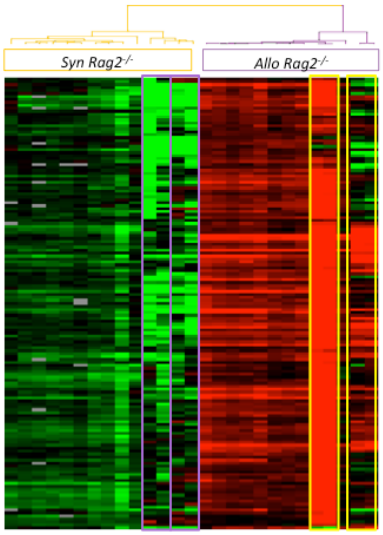

Figure 9: Gene expression analysis of the sclGVHD mouse. We performed gene expression microarray analyses of the skin of the sclGVHD mouse generated in Dr. Whitfield's lab for this study with data from the sclGVHD taken from Greenblatt et al. 2012 [9]. We find that samples from mice generated in this project (highlighted boxes) faithfully recapitulate the aberrant gene expression observed in our original study. These gene expression data are consistent with what we observe in the inflammatory subset of SSc.

Skin tissue was minced, digested with collagenase D and DNase I, and filtered through 70- and 40-micron mesh to facilitate cell dispersion. Single cell suspensions were stained with antibodies directed against the pan-leukocyte marker CD45, myeloid cell markers CD11b and CD11c, and CD115, CD206, and murine MHC-Class II (IA/IE) for flow cytometric analysis (Figure 10). Gating of positively stained cells was determined using fluorescence-minus-one (FMO) controls. CD45 positive live cells were gated and surface expression of CD11c, which is a murine dendritic cell marker, and CD11b, which is highly expressed on mouse macrophages, was analyzed on the $CD45^+$ cell population (Figures 10A and 10B). Consistent with previous reports [9, 10], there is an increase in skin macrophages ($CD11b^+CD11c^-$) in sclGVHD mice compared with syngeneic transplant controls. As demonstrated in Figure 10C, the macrophage cell population is characterized by significantly increased expression of the CSF-1R CD115 and murine MHC Class II (IA/IE). Surface levels of the mannose receptor CD206 were also elevated, although they did not reach statistical significance. These findings are consistent with results obtained by Greenblatt et al., indicating that we have established this model for our future analysis. Furthermore, these results suggest that the activation profile of SSc macrophages is unlikely to conform to a uniformly pro- or anti-inflammatory polarization state, as CD115 and CD206 are typically expressed by alternatively activated macrophages and enhanced IA/IE surface levels are characteristic of pro-inflammatory macrophages.

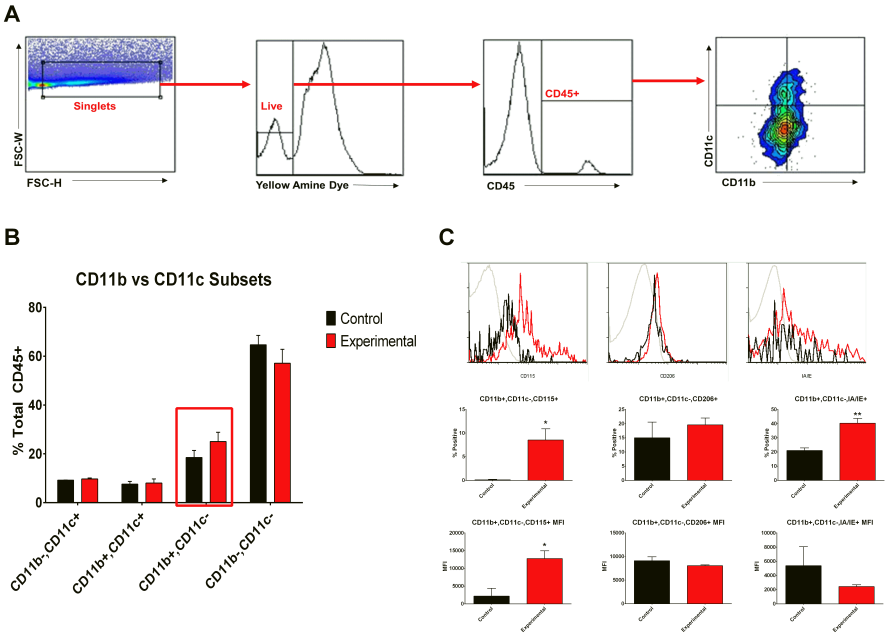

Figure 10. Characterization of the Myeloid Cell Population in skin of the 2 week old sclGVHD mouse. Flow cytometric analysis of $CD45^+$ cells derived from back skin of BALB/c *Rag2*$^{-/-}$ hosts that received either syngeneic BALB/c or allogeneic B10.D2 splenocytes two weeks prior to cell harvest (n=3 per group): A. Gating strategy for selection of CD11b vs. CD11c positive cells. B. Percentage of CD11b/CD11c cell populations in syngeneic (control) vs. allogeneic (experimental) recipients measured in panel A. and C. Percentages and mean fluorescence intensity (MFI) of three characteristic macrophage markers (CD115, CD206, and IA/IE) on gated macrophage population ($CD11b^+/CD11c^-$) in syngeneic (black bars) vs. allogeneic (red bars) recipients.

Task 4: Identify the secreted mediators of fibrosis / inflammation being produced (Whitfield / Pioli). Once cells are isolated, we will screen for secreted pro-fibrotic mediators.

We have analyzed profibrotic mediators in these cells, work is ongoing.

Task 5: Apply protocols to characterize the inflammatory infiltrate in the skin of SSc patients.

Protocols for isolating these cells from mouse skin have been optimized. Work is underway for human skin.

Milestone 3: Determine if SSc patients have a specific immune response against *R. glutinis* that is different from healthy controls and if this response can drive fibrosis.

Task 1: Test patient sera for cross-reactivity against *R. glutinis* antigens. In these experiments, we set out to test the hypothesis that autoantibody reactivity observed in SSc could recognize the same proteins in fungi, indicating that autoantibodies may have originated in response to fungal infection. Western blots were performed using R. glutinis, Malassezia furfur, Saccharomyces cerevisiae, and HeLa whole cell lysates (to test cross-reactivity with humans), and probed with sera collected from both healthy controls and SSc patients representing the three major autoantibody groups (Controls, CENP, TOP1, and RNAP3). Clear differences in cross-reactivity were evident between patient subsets. SSc patients showed a pattern of cross reactivity against R. glutinis lysates that was distinct from that observed in healthy controls. Among clinical autoantibody groups, a band consistent with the presence of TOP1 was seen in 3 of 4 TOP1 patients against R. glutinis and HeLa cells (Figure 7) this band was not observed in either M. furfur or S. cerevisiae, suggesting the possibility of cross-reactivity between R. glutinis and human TOP1 (Figure 7). Specific cross reactivity was also observed in CENP and RNAP3 patients; the identity of these proteins is being investigated.

Figure 11. Western blots using SSc and control Sera

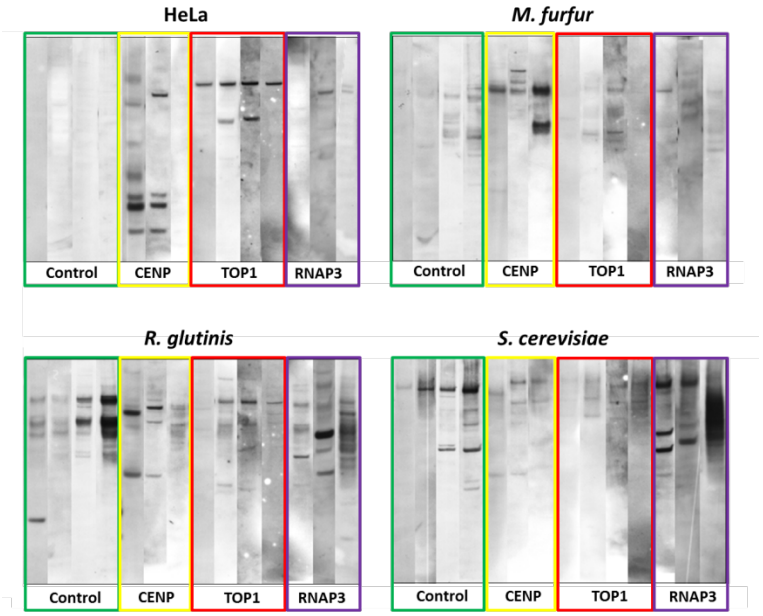

Task 2. Identify the cross-reacting proteins by mass spectrometry. Serum-immunoprecipitation of *R. glutinis* and HeLa cell whole cell lysates followed by mass spectrometry was performed to identify immunoreactive proteins associated with *R. glutinis*. As part of this investigation, we performed a high-throughput analysis of all autoantibodies present in SSc sera, revealing novel targets and associated processes associated with SSc, which is now in press (Johnson, et al. *Arthritis Research and Therapy*, 2016).

Serum-immunoprecipitation of *R. glutinis* whole cell lysates followed by mass spectrometry revealed considerable reactivity in both SSc patients and healthy controls; however, identification of target peptides was not possible due to the absence of a sufficiently well-annotated *R. glutinis* proteome. Cross reactivity of autoantibodies against human and fungal proteins has been confirmed in *S. cerevisiae*, with autoantibodies against human TOP1 strongly cross-reactive to the equivalent protein in *S. cerevisiae*.

Task 3: Use isolated PBMCs and isolated monocytes to examine the cytokines secreted and changes in gene expression when cells are exposed to *R. glutinis* or other putative micro / mycobiome triggers.

Work is underway. We have shown that PBMCs and macrophages from SSc patients (monocytes isolated from peripheral blood of SSc patients that are differentiated in autologous sera) are activated

under basal conditions, as these cells secrete pro-and anti-inflammatory mediators in the absence of exogenous activation. Therefore, additional stimulation with LPS does not appear to further activate the cells. These activated cells produce a wide range of pro-fibrotic molecules that have been implicated in SSc, including IL-6 and TGFbeta. We believe these are the major drivers of fibrosis in SSc.

Task 4: Determine if chronic exposure to *R. glutinis* or other micro / mycobiome components stimulate a fibrotic response in a mouse model of SSc.

Work underway. The sclGVHD mouse has been established and this task should be completed in the coming year.

CONCLUSION:

We have made significant progress on all milestones for the first two years of our grant. We have sequenced samples, and are actively analyzing gene expression changes and performing metagenomic analyses for micro- and mycobiome composition. Analyses of the data have revealed widespread dysbiosis in SSc skin, with additional sequencing ongoing to both confirm and expand on these results. Computational analyses have identified activated DCs and MØs as the key cell types driving the inflammatory signature, a phenotype consistent with the presence of a mycobiome trigger; these results are now being confirmed experimentally. We have generated the sclGVHD mouse model, optimized our cell isolation procedures and methods for isolating macrophages from these mice. Immuno-phenotyping and response to microbiome components is in process. We have analyzed the cross-reactivity of autoantibodies with human and fungal components. A paper reporting the autoantibody cross-reactivity to human proteins in HeLa cells has been published [11].

KEY RESEARCH ACCOMPLISHMENTS Summary

- RNA-seq followed by metagenomic analyses for microbiome components reveals dysbiosis as a common feature of SSc skin, which increases with disease duration.
- Our work has shown that the innate immune system (macrophages and DCs) are likely drivers of SSc and that these cells respond to microbiome components.
- We have successfully established the sclGVHD model in the laboratory and are examining the immune drivers and their response to microbiome components.
- Cross reactivity with microbiome component is observed and there are data to suggest basal activation of immune cells in SSc.

The next reporting period:

September 2016-September 2017

4. IMPACT

What was the impact on the development of the principal discipline(s) of the project?

The major impact of this project is that we are demonstrating a novel paradigm for the initiation of SSc. This has the potential to dramatically change the way we think about SSc and the role of the innate immune system in driving disease.

What was the impact on other disciplines?

This study impacts areas of genomics, metagenomics, microbiology, innate immunity, and autoimmunity. The methods we demonstrate and develop here will affect all of these fields. In particular, this study begins to develop methods for both systems biology and metagenomic sequencing analyses that can be used in other rare diseases.

What was the impact on technology transfer?

Technical demands associated with this project necessitated the development of a novel method to isolate DNA, RNA, and miRNAs from a single skin biopsy. This method has been submitted as a disclosure to our technology transfer office (TTO).

What was the impact on society beyond science and technology?

Scleroderma is an incurable disease that often has a very poor prognosis. If our metagenomic results are confirmed, this will provide not only a better understanding of the molecular processes driving disease pathogenesis, but also identify alternative strategies, such as anti-fungal treatment, as a possible treatment for SSc.

5. CHANGES/PROBLEMS

None to report.

6. PRODUCTS:

None at this time.

Oral Presentations: (Chronological Order)

Presentations for Michael L. Whitfield, PhD

6/16 "*Systems biology and bioinformatics approaches to evaluating disease mechanisms and therapeutic trials in autoimmunity and fibrosis*" University of North Carolina at Chapel Hill, Chapel Hill, NC

6/16 "*Burroughs Wellcome Training Program: Big Data in the Life Sciences*" Burroughs Wellcome Fund, Durham NC

5/16 "*Systems biology and bioinformatics approaches to evaluating disease mechanisms and therapeutic trials in autoimmunity and fibrosis*" University of Michigan, Rheumatology Grand Rounds, Ann Arbor MI

4/16 "*The genome and scleroderma's social network*" Scleroderma Foundation New England, Patient Education Seminar, Boston MA

3/16 "Multi-organ systems biology reveals a common immune-fibrotic axis in systemic sclerosis, pulmonary fibrosis and pulmonary arterial hypertension" Scleroderma Research Foundation Annual Workshop, San Francisco, CA

2/16 "*Systems biology and bioinformatics approaches to understand complex autoimmune diseases*" University College London, London UK

2/16 "*Integrative, multi-organ systems biology of systemic sclerosis reveals a macrophage signature associated with disease severity in multiple end-target tissues*" Scleroderma World Congress, Lisbon Portugal

2/16 "*Systems biology and bioinformatics approaches to understand complex autoimmune diseases*" Pittsburgh School of Medicine, Pittsburgh, PA

2/16 "*Advances in understanding pathogenesis and treatment in systemic sclerosis*" Rheumatology Grand Rounds, Dartmouth-Hitchcock Medical Center.

12/15 "*Big Data in the Life Sciences*" North Carolina Central University, Durham, NC

12/15 "*Big Data in the Life Sciences*" North Carolina State University, Raleigh, NC

12/15 "*Big Data in the Life Sciences*" University of North Carolina, Chapel Hill, NC

11/15 "*Multi-tissue genomic networks and systems biology in systemic sclerosis*". Scleroderma Foundation Workshop, ACR Annual meeting, San Francisco CA

8/15 *"Systems Biology in Systemic Sclerosis."* Session Chair and topic introduction. Scleroderma Basic Science Workshop, Cambridge UK.

6/15 "*Defining overlapping pathology between SSc patients and commonly used mouse models of disease*" Actelion, Basel Switzerland. (*cancelled due to illness*)

6/15 "*Genomic and Proteomic Quantification of the Heterogeneity of SSc: Implications for Pathogenesis and Treatment*". EULAR. Rome, Italy. (*cancelled due to illness*)

6/15 "*Genomics, Bioinformatics and Systems Biology for Precision Medicine in Systemic Sclerosis*". NIH CORT (P50) Advisory Committee meeting. Boston University Medical Center, Boston MA

4/15 "*Genomics, Bioinformatics and Systems Biology for Precision Medicine in Systemic Sclerosis*". SScores (NIH P30) Advisory Committee meeting. Boston University Medical Center, Boston MA.

3/15 "*A macrophage-associated inflammatory signature is found in all SSc tissues and associated with more severe disease*" Scleroderma Research Foundation Workshop on Scleroderma, San Francisco, CA

3/15 "*Molecular stratification and drug response for SSc clinical trials*" Pfizer, Cambridge, MA.

2/15 "*Enabling Precision Medicine in SSc Clinical Trials*" Discussion leader and presenter, NIAMS roundtable discussion on Scleroderma: Advancing Potential Drugs to Patient Care

2/15 "*Linking autoimmune systemic sclerosis and cancer: disease stratification, co-expression networks and genetic polymorphisms*" Cancer Mechanisms Program, Norris Cotton Cancer Center.

1/14 "*Mechanisms of Systemic Sclerosis (Scleroderma) pathogenesis by systems level genomic analyses*" Genomic Medicine Grand Rounds, Geisel School of Medicine.

12/14 "*Untangling molecular changes in SSc clinical trials: Gene expression subsets, response signatures and pathway changes*" ASSET Investigator Meeting. University of Michigan, MI

11/14 "*Identification of the Microbiome As a Potential Trigger of Systemic Sclerosis By Metagenomic RNA-Sequencing of Skin Biopsies*" ACR Basic Research Conference Boston, MA.

Dr. Sarah Arron reports no presentations on this topic in the past year.

Abstracts and Presentations: (Chronological Order)

1. Michael E. Johnson, Zhenghui Li, Michelle T. Dimon, Tammara A. Wood, Robert Lafyatis, Sarah T. Arron, **Michael L. Whitfield.** Identification of the microbiome as a potential trigger of systemic sclerosis by metagenomic RNA-sequencing of skin biopsies. American College of Rheumatology Annual Meeting, 2014

2. Zhenghui Li, Eleni Marmarelis, Kun Qu, Lionel Brooks, Patricia A. Pioli, Howard Y. Chang, Robert Lafyatis, and **Michael L. Whitfield**. RNA-seq and miR-seq analysis of SSc skin across intrinsic gene expression subsets shows differential expression of non-coding RNAs regulating SSc gene expression. American College of Rheumatology Annual Meeting, 2014

Manuscripts:

The following manuscripts from Dr. Whitfield's lab have relevance to this proposal. Publication 5 directly derives from work performed to accomplish the aims of this proposal.

1. Arron ST*, Dimon MT, Li Z, Johnson ME, Wood T., Feeney L, Angeles JG, Lafyatis R, **Whitfield ML***. High *Rhodotorula* sequences in skin transcriptome of patients with diffuse systemic sclerosis. J. Invest Derm. 2014, Mar 7. doi: 10.1038/jid.2014.127.
2. Johnson ME, Mahoney JM, Marmarelis E, Sargent JR, Wu MR, Spotts K, Hinchcliff M, **Whitfield ML***. Experimentally-derived fibroblast gene signatures identify molecular pathways associated with distinct subsets of systemic sclerosis patients in three independent cohorts. PLoS One. 2015 Jan 21;10(1):e0114017. doi: 10.1371/journal.pone.0114017. eCollection 2015.
3. Mahoney JM, Taroni J, Martyanov V, Wood TA, Greene CS, Pioli PA, Hinchcliff M, **Whitfield ML***. Systems level analysis of systemic sclerosis shows a network of immune and profibrotic pathways connected with genetic polymorphisms. PLoS Comput Biol. 2015 Jan 8;11(1):e1004005. doi: 10.1371/journal.pcbi.1004005. eCollection 2015 Jan.
4. Taroni JN, Martyanov V, Wood TA, Choe S, Huang CC, Hirano I, Yang GY, Brenner D, Jung B, Carns M, Podluski S, Chang RW, Varga J, **Whitfield ML**, Hinchcliff M. Genome-wide gene expression analysis of systemic sclerosis esophageal biopsies identifies disease-specific molecular subsets. Arthritis Res Ther. 2015 Jul 29;17:194. doi: 10.1186/s13075-015-0695-1
5. Michael E. Johnson, Andrew V. Grassetti, Jaclyn N. Taroni, Shawn M. Lyons, Devin Schweppe, Jessica K. Gordon, Robert F. Spiera, Robert Lafyatis, Paul J. Anderson, Scott A. Gerber, **Michael L. Whitfield**. Stress Granules and RNA Processing Bodies are Novel Autoantibody Targets in Systemic Sclerosis. Arthritis Res Ther. 2016 Jan 22;18:27. doi: 10.1186/s13075-016-0914-4.
6. Sargent JL, Li Z, Aliprantis AO, Greenblatt M, Lemaire R, Wu MH, Wei J, Taroni J, Harris A, Long KB, Burgwin C, Artlett CM, Blankenhorn EP, Lafyatis R, Varga J, Clark SH, **Whitfield ML**. Identification of Optimal Mouse Models of Systemic Sclerosis by Interspecies Comparative Genomics. Arthritis Rheumatol. 2016 Aug;68(8):2003-15. doi: 10.1002/art.39658
7. Martyanov V, **Whitfield ML**. Molecular stratification and precision medicine in systemic sclerosis from genomic and proteomic data. Curr Opin Rheumatol. 2016 Jan;28(1):83-8. doi: 10.1097/BOR.0000000000000237. Review.
8. Zhenghui Li, Guoshuai Cai, Michael S. Ball, Kun Qu, Patricia A. Pioli, Howard Chang, Sarah Arron, Robert Lafyatis, and **Michael L. Whitfield**. Functional Characterization of Systemic Sclerosis Transcriptome Identifies a Coding Region Polymorphism more Prevalent in Africans that affects IL6 Production. *In preparation*

The following additional papers were published by Drs. Whitfield, Lafyatis and Arron during the funding period.

1. Long KB, Li Z, Burgwin C, Cho SG, Martyanov V, Sassi-Gaha S, Earl J, Eutsey R, Ahmed A, Ehrlich GD, Artlett CM, **Whitfield ML**, Blankenhorn EP *. The Tsk2/+ mouse fibrotic phenotype is due to a gain-of-function mutation in the PIIINP segment of the *Col3a1* gene. J. Invest Derm. 2014, Oct 20. doi: 10.1038/jid.2014.455.
2. Iwamoto N, Vettori S, Maurer B, Brock M, Jüngel A, Calcagni M, Gay RE, **Whitfield ML**, Distler J.H.W, Gay S, Distler O*. Downregulation of miR-193b in systemic sclerosis regulates the proliferative vasculopathy by urokinase-type plasminogen activator expression. Ann Rheum Dis. 2014 Nov 10. pii: annrheumdis-2014-205326. doi: 10.1136/annrheumdis-2014-205326. [Epub ahead of print]
3. Marangoni RG, Korman B, Wei J, Wood TA, **Whitfield ML,** Scherer PE, Tourtellotte WG and Varga J*. Myofibroblasts in Cutaneous Fibrosis Originate from Intradermal Adipocytes. Arthritis Rheumatol. 2015 Apr;67(4):1062-73. doi: 10.1002/art.38990.
4. Chakravarty EF, Martyanov V, Fiorentino D, Wood TA, Haddon DJ, Jarrell JA, Utz PJ, Genovese MC, **Whitfield ML**, Chung L. A Pilot Randomized Placebo-Controlled study of Abatacept for the Treatment

of Diffuse Cutaneous Systemic Sclerosis. Arthritis Research & Therapy, Arthritis Res Ther. 2015 Jun 13;17(1):159.

5. Fresolimumab treatment decreases biomarkers and improves clinical symptoms in systemic sclerosis patients. Rice LM, Padilla CM, McLaughlin SR, Mathes A, Ziemek J, Goummih S, Nakerakanti S, York M, Farina G, **Whitfield ML**, Spiera RF, Christmann RB, Gordon JK, Weinberg J, Simms RW, Lafyatis R. J. Clin. Invest. 2015 Jun 22. pii: 77958. doi: 10.1172/JCI77958
6. Lisa M. Rice, Jessica Ziemack, Eric Stratton, Sarah Mclauglin, Cristina Padilla, Allison Mathes, Romy Christmann, Giuseppina Stifano, Jeff Browning, **Michael L. Whitfield**, Robert Spiera, Jessica Gordon, Robert Simms, Yuqing Zhang, Robert Lafyatis. A longitudinal biomarker for the extent of skin disease in patients with diffuse cutaneous systemic sclerosis. Arthritis Rheumatol. 2015 Nov;67(11):3004-15. doi: 10.1002/art.39287.
7. Gordon JK, Martyanov V, Wood TA, Spiera RF, **Whitfield ML.** Nilotinib (Tasigna™) in the Treatment of Early Diffuse Systemic Sclerosis: An Open-Label, Pilot Clinical Trial. Arthritis Res Ther. 2015 Aug 18;17:213. doi: 10.1186/s13075-015-0721-3.
8. Brooks L, Lyons SM, Mahoney JM, Welch JD, Liu Z, Marzluff WF, and **Whitfield ML**. A multi-protein occupancy map of the histone mRNP. RNA. 2015 Nov;21(11):1943-65. doi: 10.1261/rna.053389.115. Epub 2015 Sep 16.
9. Lyons SM, Cunningham CH, Welch JD, Groh B, Guo AY, Wei B, **Whitfield ML**, Xiong Y, Marzluff WF. A subset of replication-dependent histone mRNAs are expressed as polyadenylated RNAs in terminally differentiated tissues. Nucleic Acids Res. 2016 Jul 8. pii: gkw620.

Degrees obtained that are supported by this award

Dr. Zhenghui Li, who worked on the microbiome project, will complete his Ph.D during year 2 of funding. He has received direct support from this grant.

Development of cell lines, tissue or serum repositories

None

7. PARTICIPANTS & OTHER COLLABORATING ORGANIZATIONS

None

8. SPECIAL REPORTING REQUIREMENTS

COLLABORATIVE AWARDS: For collaborative awards, independent reports are required from BOTH the Initiating PI and the Collaborating/Partnering PI. A duplicative report is acceptable; however, tasks shall be clearly marked with the responsible PI and research site. A report shall be submitted to https://ers.amedd.army.mil for each unique award.

An identical final progress report will be sent from Dr. Arron

9. REFERENCES

1. Johnson M, Mahoney J, Taroni J, Sargent J, Marmarelis E, Wu M, Varga J, Hinchcliff M, Whitfield M: **Experimentally-derived fibroblast gene signatures identify molecular pathways associated with distinct subsets of systemic sclerosis patients in three independent cohorts.** *PLoS ONE* 2015, **10:**e0114017.
2. Whitfield ML, Finlay DR, Murray JI, Troyanskaya OG, Chi JT, Pergamenschikov A, McCalmont TH, Brown PO, Botstein D, Connolly MK: **Systemic and cell type-specific gene expression patterns in scleroderma skin.** *Proc Natl Acad Sci U S A* 2003, **100:**12319-12324.

3. Milano A, Pendergrass SA, Sargent JL, George LK, McCalmont TH, Connolly MK, Whitfield ML: **Molecular subsets in the gene expression signatures of scleroderma skin.** *PLoS ONE* 2008, **3:**e2696.
4. Pendergrass SA, Lemaire R, Francis IP, Mahoney JM, Lafyatis R, Whitfield ML: **Intrinsic gene expression subsets of diffuse cutaneous systemic sclerosis are stable in serial skin biopsies.** *J Invest Dermatol* 2012, **132:**1363-1373.
5. Hinchcliff M, Huang CC, Wood TA, Matthew Mahoney J, Martyanov V, Bhattacharyya S, Tamaki Z, Lee J, Carns M, Podlusky S, et al: **Molecular signatures in skin associated with clinical improvement during mycophenolate treatment in systemic sclerosis.** *J Invest Dermatol* 2013, **133:**1979-1989.
6. Taroni JN, Martyanov V, Huang CC, Mahoney JM, Hirano I, Shetuni B, Yang GY, Brenner D, Jung B, Wood TA, et al: **Molecular characterization of systemic sclerosis esophageal pathology identifies inflammatory and proliferative signatures.** *Arthritis Res Ther* 2015, **17:**194.
7. Arron ST, Dimon MT, Li Z, Johnson ME, T AW, Feeney L, J GA, Lafyatis R, Whitfield ML: **High Rhodotorula sequences in skin transcriptome of patients with diffuse systemic sclerosis.** *J Invest Dermatol* 2014, **134:**2138-2145.
8. Mahoney JM, Taroni J, Martyanov V, Wood TA, Greene CS, Pioli PA, Hinchcliff ME, Whitfield ML: **Systems level analysis of systemic sclerosis shows a network of immune and profibrotic pathways connected with genetic polymorphisms.** *PLoS Comput Biol* 2015, **11:**e1004005.
9. Greenblatt MB, Sargent JL, Farina G, Tsang K, Lafyatis R, Glimcher LH, Whitfield ML, Aliprantis AO: **Interspecies comparison of human and murine scleroderma reveals IL-13 and CCL2 as disease subset-specific targets.** *Am J Pathol* 2012, **180:**1080-1094.
10. Zhang Y, McCormick LL, Desai SR, Wu C, Gilliam AC: **Murine sclerodermatous graft-versus-host disease, a model for human scleroderma: cutaneous cytokines, chemokines, and immune cell activation.** *J Immunol* 2002, **168:**3088-3098.
11. Johnson ME, Grassetti AV, Taroni JN, Lyons SM, Schweppe D, Gordon JK, Spiera RF, Lafyatis R, Anderson PJ, Gerber SA, Whitfield ML: **Stress granules and RNA processing bodies are novel autoantibody targets in systemic sclerosis.** *Arthritis Res Ther* 2016, **18:**27.

10. APPENDIX

1. Michael E. Johnson, Andrew V. Grassetti, Jaclyn N. Taroni, Shawn M. Lyons, Devin Schweppe, Jessica K. Gordon, Robert F. Spiera, Robert Lafyatis, Paul J. Anderson, Scott A. Gerber, Michael L. Whitfield. Stress Granules and RNA Processing Bodies are Novel Autoantibody Targets in Systemic Sclerosis, Arthritis Res Ther. 2016 Jan 22;18:27. doi: 10.1186/s13075-016-0914-4.

Johnson et al. Arthritis Research & Therapy (2016) 18:27
DOI 10.1186/s13075-016-0914-4

Arthritis Research & Therapy

RESEARCH ARTICLE Open Access

Stress granules and RNA processing bodies are novel autoantibody targets in systemic sclerosis

Michael E. Johnson[1], Andrew V. Grassetti[1], Jaclyn N. Taroni[1], Shawn M. Lyons[2], Devin Schweppe[1], Jessica K. Gordon[3], Robert F. Spiera[3], Robert Lafyatis[4], Paul J. Anderson[2], Scott A. Gerber[1] and Michael L. Whitfield[1,5*]

Abstract

Background: Autoantibody profiles represent important patient stratification markers in systemic sclerosis (SSc). Here, we performed serum-immunoprecipitations with patient antibodies followed by mass spectrometry (LC-MS/MS) to obtain an unbiased view of all possible autoantibody targets and their associated molecular complexes recognized by SSc.

Methods: HeLa whole cell lysates were immunoprecipitated (IP) using sera of patients with SSc clinically positive for autoantibodies against RNA polymerase III (RNAP3), topoisomerase 1 (TOP1), and centromere proteins (CENP). IP eluates were then analyzed by LC-MS/MS to identify novel proteins and complexes targeted in SSc. Target proteins were examined using a functional interaction network to identify major macromolecular complexes, with direct targets validated by IP-Western blots and immunofluorescence.

Results: A wide range of peptides were detected across patients in each clinical autoantibody group. Each group contained peptides representing a broad spectrum of proteins in large macromolecular complexes, with significant overlap between groups. Network analyses revealed significant enrichment for proteins in RNA processing bodies (PB) and cytosolic stress granules (SG) across all SSc subtypes, which were confirmed by both Western blot and immunofluorescence.

Conclusions: While strong reactivity was observed against major SSc autoantigens, such as RNAP3 and TOP1, there was overlap between groups with widespread reactivity seen against multiple proteins. Identification of PB and SG as major targets of the humoral immune response represents a novel SSc autoantigen and suggests a model in which a combination of chronic and acute cellular stresses result in aberrant cell death, leading to autoantibody generation directed against macromolecular nucleic acid-protein complexes.

Keywords: Systemic sclerosis, Scleroderma, Autoantibody, RNA processing bodies, Stress granules

Background

Systemic sclerosis (SSc) is a rare systemic autoimmune disease of unknown etiology characterized by skin fibrosis, internal organ involvement, vascular abnormalities, and autoantibody production. Patients are broadly classified as having either limited (lSSc) or diffuse (dSSc) disease based primarily upon the extent of skin involvement and autoantibody profiles. While a wide array of autoantibodies have been described for SSc, only a small number of these targets are used for clinical diagnosis and stratification. Autoantibodies targeting RNA polymerase III (RNAP3), topoisomerase 1 (TOP1; commonly referred to as Scl70), and centromere proteins (CENP) represent the three the most common, clinically measured autoantibodies observed in SSc [1, 2]. Other autoantibodies, including fibrillarin (U3RNP), Pm/Scl, Ku, U1RNP, U11/U12, and Th/To have also been described [1, 3] but are not routinely measured for clinical subtyping.

* Correspondence: michael.l.whitfield@dartmouth.edu
[1]Department of Genetics, Geisel School of Medicine at Dartmouth, Hanover, NH, USA
[5]Dartmouth Medical School, Hinman Box 7400, Hanover, NH 03755, USA
Full list of author information is available at the end of the article

While the processes underlying autoantibody production in SSc remain poorly understood, the presence of certain autoantibodies is strongly predictive of clinical outcomes [1–3]. TOP1 and RNAP3 autoantibodies are almost exclusively seen in dSSc, while CENP, Th/To, and U1RNP antibodies are more commonly associated with lSSc [1, 3]. U3RNP autoantibodies are not associated with either clinical subset, and are often found in conjunction with other autoantibodies, including both TOP1 and CENP [3]. Certain antibodies, such as TOP1 and U11/12, have been shown to be predictive of poorer overall prognosis, including increased likelihood of pulmonary fibrosis [4] and cardiac involvement, while RNAP3 autoantibodies have recently been linked to co-occurrence of SSc with cancer [5].

Despite the importance of autoantibodies in SSc, the vast majority of target identification and phenotypic screening has been performed using methods targeting only a single autoantibody, with little ability to detect novel or low abundance autoantibodies. Furthermore, these methods fail to address the possibility of co-occurrence of multiple autoantibodies within a patient, which may have important clinical implications. Autoantigen microarrays have proven successful for screening large numbers of autoantibodies in parallel, however target identification is limited to those antigens produced and printed on the antigen microarrays [6]. To address these limitations, we performed immunoprecipitations (IP) of HeLa whole cell lysates using sera from RNAP3-, CENP-, and TOP1-positive patients, as well as healthy controls, followed by mass spectrometry (LC-MS/MS) to provide an unbiased assessment of all autoantibodies present in these SSc patients. This method provides a better view of the full range of autoantibodies present in SSc, including both novel and established targets, and provides insights into the general processes underlying autoantibody production.

Methods

Clinical samples

Patient serum was obtained from Boston University Medical School, Boston (BUMC), MA, USA and the Hospital for Special Surgery (HSS), New York, NY, USA. All relevant study protocols were approved by the Dartmouth College committee for the protection of human subjects, and the internal review boards of both BUMC and HSS. Informed consent was obtained from all patients prior to sample collection. Patients were diagnosed with either dSSc or limited SSc, as determined using the 1980 American College of Rheumatology classification criteria. Detection of major autoantibody reactivities was performed using standard clinical assays.

Human cell lysates

HeLa cells were cultured in DMEM supplemented with 10 % fetal bovine serum (FBS) (v/v) and 100 IU/mL penicillin-streptomycin. Cells were grown to approximately 80 % confluence, harvested in IP lysis buffer (150 mM NaCl, 50 mM Tris pH 7.5, 1 mM $MgCl_2$, 1 mM EDTA, 0.5 % Triton X-100, 2.5 mM β-mercaptoethanol, 1 mM sodium molybdate, 1 mM sodium fluoride, 1 mM sodium tartrate, 1 mM dithiothreitol (DTT), and protease inhibitors (Roche, Indianapolis, IN, USA)), lysed by passage through a pre-chilled high-gauge syringe, and centrifuged for 15 minutes to pellet debris. Lysates were then clarified by incubating for 4 h at 4 °C on a rotating platform. Protein concentrations were quantified using a standard bicinchoninic acid (BCA) protein assay kit (Thermo Scientific, Waltham, MA, USA).

Serum immunoprecipitation

Patient serum was cross-linked to Protein G Dynabeads (Invitrogen, St. Louis, MO, USA) prior to IP. First, 100 μL serum (approximately 1 mg IgG) was added to 50 μL Protein G beads and incubated for 5 h at 4 °C. Samples were then washed in PBS, equilibrated in crosslinking buffer (50 mM HEPES, pH 8.2), and cross-linked to Protein G beads by the addition of 20 mM dimethyl pimelimidate and 300 mM HEPES (DMP) solution for 10 minutes at room temperature (repeated three times). The crosslinking reaction was then terminated by the addition of 50 mM ammonium bicarbonate, and the resulting antibody bead mixture added to 500 μL cell lysate (diluted to 4 mg/mL in IP lysis buffer). Samples were incubated overnight at 4 °C on a rotating platform, washed in cold IP lysis buffer, and eluted in a buffer containing 2 % SDS, 75 mM NaCl, 50 mM Tris pH 8.1, and 20 % glycerol at 65 °C for 5 minutes. Eluates were reduced by the addition of 0.1 M dithiothreitol (DTT) (to a final concentration 5 mM), and incubated at 80 °C for 5 minutes. Samples were then resolved by SDS-PAGE, split into high (>60 kDa) and low (<60 kDa) molecular weight fractions and analyzed by mass spectrometry.

Mass spectrometry

Proteins contained in Coomassie-stained gel regions were digested overnight with trypsin (1:200 w/v) at 37 °C. Following digestion, peptides were extracted from the gels, dried, and analyzed by nanoscale LC-MS/MS. LC-MS/MS analyses were performed on either LTQ Orbitrap Classic or Orbitrap Fusion LC-MS/MS platforms. LTQ Orbitrap Classic analyses were conducted as described previously [7].

For Orbitrap Fusion analyses, samples were loaded onto an EASY-nLC 1000 Liquid Chromatograph (Thermo Scientific, Waltham, MA, USA) and separated by reverse-phase high pressure liquid chromatography (RP-HPLC)

using an approximately 36-cm column with a 100-μM inner diameter packed with 3 μm 120 Å C_{18} particles (Dr. Maisch GmbH, Ammerbuch-Entringen, Germany). The resultant peptide eluate was directed into an Orbitrap Fusion Tribrid Mass Spectrometer operating in a data-dependent sequencing acquisition mode across a 30-minute reverse-phase gradient (6 % acetonitrile, 0.1 % formic acid to 30 % acetonitrile, 0.1 % formic acid) at 350 nL/min flow rate. The Orbitrap Fusion was operated with an Orbitrap MS1 scan at 120 K resolution, followed by Orbitrap MS2 scans of higher energy collision-induced dissociation (HCD) fragment ions (30 % HCD energy) at 15 K resolution using a maximum cycle type of 2 s, precursor ion dynamic exclusion window of 15 s, +2, +3, and +4 precursor ions selected for LC-MS/MS, and maximum ion injection times of 100 ms (MS1) and 50 ms (MS2). The resulting tandem mass spectra were data-searched using the COMET search engine [8] against a *Homo sapiens* proteome database (source: Uniprot; download date: 2 July 2013) with a precursor ion tolerance of +/- 1 Da [9] and a fragment ion tolerance of 0.02 Th. Peptide spectra matches (PSMs) were filtered to <1 % false discovery rate using the target decoy strategy [10], and reported.

IP-western blots

Anti-UPF1 antibody was kindly provided by Dr. Lynne Maquat (University of Rochester Medical Center, Rochester, NY, USA). Antibodies to MOV10 and CAPRIN1 were purchased from Proteintech (Chicago, IL, USA); antibodies to G3BP1 and USP10 were purchased from Santa Cruz Biotechnology (Santa Cruz, CA, USA). Serum immunoprecipitation of HeLa lysates was performed as described above; 50 % of each eluate (15 μL) was then run on a 10 % bis-tris precast gel (Life Technologies, Carlsbad, CA, USA). HeLa whole cell lysate (100 μg) was used as a positive control; no loading control was performed due to the absence of viable targets present in all IP eluates. Western blots were then run following standard protocols, and visualized using Western Lightning ECL Pro or Ultra substrate (Perkin Elmer Inc., Waltham, MA, USA), as necessary.

Data analysis

Non-redundant peptide hits, defined as mass spectra mapping exclusively to a given peptide fragment, were used for all downstream analyses. Pairwise comparisons between samples were performed by Fisher's exact test using the Bonferroni correction for multiple hypothesis testing. Venn diagrams were generated using VENNY [11]. Network analysis was performed using the Genome-scale Integrated Analysis of gene Networks in Tissues (GIANT; http://giant.princeton.edu/) global network [12] and visualized using Cytoscape [13]. Communities in the network were detected using fast-greedy modularity as implemented in igraph. Functional annotation of individual communities was performed using g:Profiler [14]. Semiquantitative enrichment of SSc-associated autoantibodies was determined using a binary assessment of autoantibody presence or absence in a sample. Preferential enrichment in SSc was defined as all proteins detected in >50 % of all patient samples at a frequency >1.5-fold relative to controls. Enrichment of biological processes and cellular components was determined using g:Profiler using the g:SCS threshold correction for multiple hypothesis testing and a functional category size ≤500 genes. Hierarchical clustering was performed using Cluster 3.0 [15], and visualized using Java TreeView [16].

Immunofluorescence

The day prior to the experiment, 10^5 U2OS cells were seeded onto 11 mm glass coverslips and allowed to attach overnight at 37 °C/5 % CO_2 in DMEM containing 10 % FBS (Gibco). Cells were treated with 100 μM sodium (meta)arsenite (Sigma Aldrich) for 1 h to induce the formation of stress granules and then with 4 % paraformaldehyde solution at room temperature for 15 - minutes followed by blocking and permeabilization with 5 % normal horse serum, 0.1 % digitonin in Tris-buffered saline. Staining was performed with anti-eIF3b (Santa Cruz), anti-SK1-Hedls (Santa Cruz), and patient sera for 1 h at room temperature. Secondary antibodies (anti-goat-Cy3, anti-mouse-Cy2, and anti-human-Cy5) were purchased from Jackson Laboratories and incubated at room temperature for 1 h. Conventional fluorescence microscopy was performed using a microscope (model Elipse E800, Nikon, Tokyo, Japan) with epifluorescence optics with a digital camera (model CCD-SPOT RT; Diagnostic Instruments, Sterling Heights, MI). Images were compiled using Adobe Photoshop software (CS6; Adobe Systems, San Jose, CA).

Results

Identification of proteins cross-reacting to serum antibodies

Immunoprecipitations (IP) of HeLa whole cell lysates were performed using sera obtained from 13 SSc patients and 4 healthy controls. HeLa cells were chosen based upon their consistent, high level of expression of a broad range of proteins from the human genome [17].

SSc patients were divided into three groups, TOP1, RNAP3, and CENP, as measured in a reference laboratory; clinical data for each patient are shown in Table 1. These groups were chosen based upon their relative frequency, and their importance in clinical diagnosis. Immunoprecipitated proteins were analyzed by LC-MS/MS, and the resulting spectra aligned to the reference human proteome (UCSC version hg19). Data are presented in two ways; first to identify the total number of

Table 1 Clinical information for patients involved in this study

Sample	Group	Age (years)	Sex	Race	Disease type	ILD/PAH	Disease duration (years)	ANA pattern	ANA titer	MRSS
SSc 1	TOP1	36	F	White	Diffuse	mild ILD	2.5		1:320	43
SSc 132	TOP1	49	F	White	Diffuse	No		Homogeneous	1:640	27
SSc 218	TOP1	55	F	White	Diffuse	ILD		Homogeneous/nucleolar	1:2560	18
SSc 208	TOP1	64	M	White	Diffuse	No		Nucleolar	1:1280	37
SSc 5	RNAP3	53	M	White	Diffuse	No	0.75	Speckled	1:80	36
SSc 7	RNAP3	45	F	Black	Diffuse	No	0.5	Speckled	1:80	27
SSc 10	RNAP3	52	M	White	Diffuse	No	0.5		0	22
SSc 18	RNAP3	69	F	White	Diffuse	ILD	0.5	Nucleolar	1:160	44
SSc 159	CENP	54	F	Mixed	Limited	No	7	Centromere	1:1280	2
SSc 177	CENP	64	F	White	Limited	No	15	Discrete speckled	4+	
SSc 194	CENP	66	F	White	Limited	No	18	Discrete speckled	4+	6
SSc 238	CENP	53	F	White	Limited	No	6	Centromere	1:640	5
SSc 226	CENP	55	F	Asian	Diffuse	No		Centromere	1:1280	6
HC 162	Control	24	M	White						
HC 400	Control	21	M	White						
HC 117	Control		M							
HC 118	Control		M							

Blank cells indicate information not available at the time of sample collection. *ILD* interstitial lung disease, *PAH* pulmonary arterial hypertension, *ANA* anti-nuclear antibody, *MRSS* modified Rodnan skin score, *SSc* systemic sclerosis, *M* male, *F* female

peptides that could be aligned to each protein (total hits), and second to identify all non-redundant peptides that mapped exclusively to a given protein (non-redundant hits). A complete list of all data can be found in Additional file 1: Table S1.

Exclusivity and co-occurrence of SSc autoantibodies

We observed a high degree of reproducibility between patients within their respective autoantibody groups (TOP1, RNAP3, and CENP; Fig. 1). The greatest degree of overlap between peptides was observed among RNAP3 patients (Fig. 1a and c), with 420 proteins (54.1 %) detected in all four patients (Fig. 1c). The remaining groups exhibited significant overlap in three of four (TOP1) and four of five (CENP) patients, respectively (Fig. 1a), along with a single outlier that showed either higher (SSc 208; TOP1) or lower (SSc 226; CENP) total peptide hits relative to other samples in these groups. Within TOP1, 111 proteins (14.2 %) were detected in all four patients (Fig. 1d), while CENP exhibited 48 proteins (10.5 %) common to all patients (Fig. 1c). The least overlap was seen in healthy controls, with only 40 proteins (7.6 %; Fig. 1b) common across individuals.

Across all samples, 283 proteins (25.0 %) were detected in at least one patient in each of the four autoantibody groups (Fig. 1e, Additional file 2: Table S2). Some of these proteins likely represent background signals (serum albumin (ALB), β-tubulin (TUBB), and ribosomal proteins), while others are considered specific to SSc despite trace level detection in controls. For example, multiple SSc autoantibody targets, including Ku (XRCC5 and XRCC6), Ro52/TRIM21, and nucleophosmin/B23 (NPM1) were present in this set of proteins. In contrast, 87 proteins (7.7 %) were detected in all three SSc groups, but were absent in controls (Fig. 1e; Additional file 2: Table S2). Functional analyses of these proteins revealed strong enrichment of proteins involved in oxidative stress responses and nucleic acid processing (Additional file 3: Table S3B).

Of the 1,130 non-redundant proteins identified, 473 (41.8 %) were unique to a given autoantibody group (Fig. 1f); however, the vast majority of these proteins were exclusive to a single patient, with only 111 (23.5 %) detected in two or more patients. These results suggest a wide range of autoantibody responses within each of the clinical autoantibody groups beyond what has already been described.

Among the major autoantibody groups, immunoprecipitation of RNAP3 was exclusive to the RNAP3 group, with no RNAP3 peptides detected in any of the other samples (Table 2). In contrast, TOP1 peptides were consistently highest among TOP1 patients, but were also detected at low levels in all four RNAP3$^+$ patients, and in two controls (Table 2). As these patients were negative for TOP1 autoantibodies by clinical testing, these results indicate a higher degree of sensitivity for our IP/MS protocol compared to standard ELISA-based methods used clinically. In contrast, CENP was only

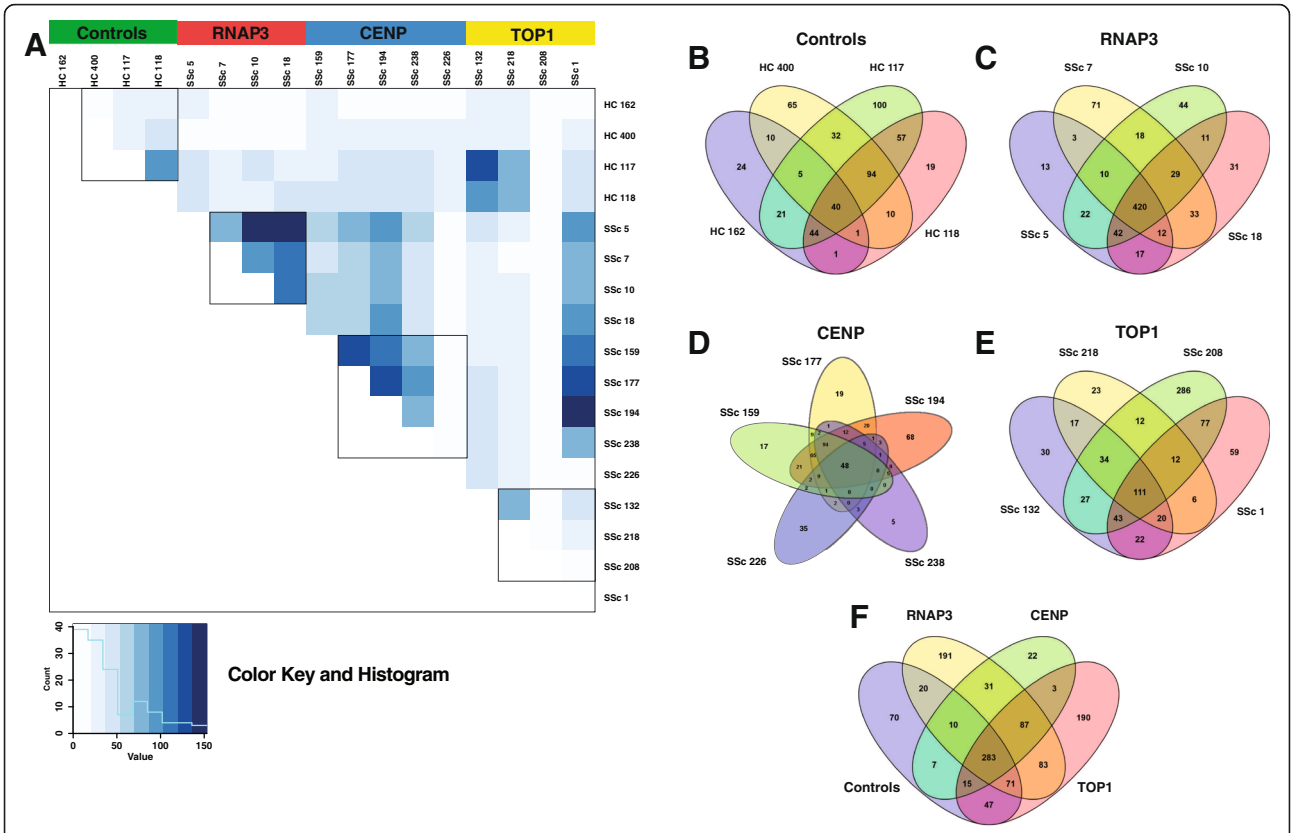

Fig. 1 Overview of mass spectrometry results. **a** Correlation matrix of non-redundant protein hits for all patients and controls. Comparisons were performed using Fisher's exact test with the Bonferroni correction. *Black boxes* indicate intra-group comparisons for each of the four clinically defined groups. *Green* controls; *red* RNA polymerase III (*RNAP3*); *blue* centromere protein (*CENP*); *yellow* topoisomerase I (*TOP1*). **b-f** *Venn diagrams* depict overlap in non-redundant peptide hits within and between groups. **b** healthy controls, **c** RNAP3, **d** CENP, **e** TOP1, and **f** overlap between groups

detected at low levels in the CENP group, likely because it remained bound to the tightly packed centromere complex of chromatin.

Other known SSc autoantigens were also detected. RuvBL [18] was strongly detected in all SSc samples, while virtually absent in controls. Ku and Su, along with a wide array of anti-tRNA synthetases [19] were routinely detected in both the RNAP3 and TOP1 subsets, but were only weakly present in the CENP and control groups (Table 2).

Several autoantigens previously implicated in SSc were found at low, background levels in both SSc and control samples. Ro52/TRIM21 [20] and nucleophosmin/B23 [21] were widely detected across all four groups, suggesting widespread reactivity to these proteins in SSc and controls. We did not find evidence in SSc of enrichment of Pm/Scl autoantibodies, which target exosome components EXOSC1-10 [22]. Peptides for these proteins were absent in the CENP group, but were detected at low levels in other subsets, including controls. Autoantigens not detected here include many of the URNPs, PDGFR, matrix metalloproteinases, tissue plasminogen activator, and vascular receptor antibodies (Table 2).

Functional clustering of identified proteins

To identify functional interactions among autoantigens, all 763 non-redundant protein hits were submitted as a query to the GIANT global average network. This approach included both SSc-specific targets and those detected at background levels in controls, to better understand the full range of autoreactive proteins and complexes. Nine distinct communities were identified within the resulting network, in which each gene is represented by a node, and two genes share an edge if they are predicted to functionally interact (Additional file 4: Figure S1). Analysis of each of these communities by g:Profiler revealed functional enrichment for a wide range of biological processes associated with important disease processes and components (Additional file 4: Figure S1). Community 1 is dominated by ribosomal proteins, eukaryotic initiation factor 3 (eIF3) subunits, and includes the SSc autoantibody target nucleophosmin/B23. Communities 2 and 8 show strong enrichment for Gene Ontology (GO) terms mRNA processing, ribonucleoprotein complex, and cytosolic stress granule. Community 2 is dominated primarily by DEAD box

Table 2 SSc-associated autoantibodies observed in this study

Alias	Associated proteins	Disease subset	Clinical associations	Prevalence in this dataset (avg/freq)				Reference
				Control (n = 4)	RNAP3 (n = 4)	TOP1 (n = 4)	CENP (n = 5)	
Major autoantibodies								
RNA Pol III	POLR3A	dSSc	Renal crisis, cancer	-	+++ (28/4)	-	-	Graf, et al. 2012 [1]; Mehra, et al. 2013 [3]
Scl70	TOP1	dSSc	Poor prognosis, internal organ involvement, and proteinuria	+ (3/2)	+ (4/4)	+++ (19/4)	-	Mehra, et al. 2013 [3]
Centromere	**CENPB**, CENPH	lSSc/CREST	PAH, ILD	-	-	-	+ (1/2)	Mehra, et al. 2013 [3]
Other SSc autoantibodies present in our dataset								
Endothelial Cell	TUBB, **VCL**, LMNA, RPLP0	SSc	PAH	+ (1/1)	++ (6/4)	+ (4/2)	+ (0/1)	Dib, et al. 2012 [34], Naniwa, et al. 2007 [35]
Fibroblast	ENO1, G6PD, **HSPA1A**, HSPA1B, VIM	SSc	PAH	+ (3/4)	+++ (12/4)	++ (5/3)	++ (8/5)	Terrier, et al. 2008 [36], Terrier, et al. 2009 [37]
Histone	H1FX, HIST1H1B, **HIST1H4A**	SSc	PF, internal organ involvement, decreased survival	+ (1/1)	+ (3/3)	+ (1/1)	-	Mehra, et al. 2013 [3]
B23	NPM1	dSSc, CENP- lSSc	PAH	+ (4/4)	++ (7/4)	++ (5/4)	++ (6/5)	Mehra, et al. 2013 [3]
Ku	**XRCC5**, XRCC6	lSSc	Myositis	+ (3/3)	+++ (12/4)	++ (8/4)	+ (2/3)	Graf, et al. 2012 [1]; Mehra, et al. 2013 [3]
Su	AGO2	SSc, PM/Scl	Unknown	-	+ (1/2)	+ (3/1)	-	Satoh, et al. 2013 [38]
Mitochondrial (M2)	**DLD**, PDHB	lSSc	Strong association with primary biliary cirrhosis	+ (1/1)	+ (2/3)	+ (1/1)	-	Mehra, et al. 2013 [13]
Pm/Scl	EXOSC1-**10**	SSc	PF, digital ulcers; decreased risk of PAH and GI symptoms	+ (2/2)	++ (5/3)	+ (2/2)	-	Mehra, et al. 2013 [13]
hnRNPs	**HNRNPA1**-3, HNRNPL	SSc	Common in SARDs	+ (0/1)	++ (7/4)	+ (3/4)	+ (2/4)	Siapka, et al. 2007 [39]
U1	**SNRNPA**, SPRNP70	SSc	Co-occurrence with SS-A/SS-B, PAH, overlap syndrome	-	+ (2/4)	+ (1/2)	+ (0/1)	Graf, et al. 2012 [1]; Mehra, et al. 2013 [3]
U5	SNRNP200	SSc, PM/Scl	Unknown	++ (6/3)	++ (9/4)	++ (8/3)	+ (1/2)	Kubo, et al. 2002 [40]
RO52/TRIM21	TRIM21	SSc	ILD, other autoimmune diseases	++ (6/3)	+++ (12/4)	++ (6/4)	++ (8/4)	Mehra, et al. 2013 [3]
RuvB	**RUVBL1**, RUVBL2	dSSc	Common in SARDs, older age at onset, male sex	+ (1/1)	++ (7/4)	+ (3/4)	+ (2/4)	Kaji, et al. 2014 [18]
Annexin V	ANXA5	dSSc, CENP- lSSc	Digital ischemia	+ (2/2)	++ (7/4)	+ (4/3)	+ (3/4)	Mehra, et al. 2013 [3]
SS-B/LA	SS-A, **SS-B**	SSc	ILD, other autoimmune diseases	-	+ (3/4)	+ (2/2)	+ (0/1)	Mehra, et al. 2013 [3]
Peroxiredoxin	PRDX1	SSc	Disease duration, PF, cardiac involvement, TOP1+ patients	+ (2/4)	++ (8/4)	+ (3/3)	+ (4/4)	Mehra, et al. 2013 [3]
hUBF/NOP90	UBTF	lSSc	Mild organ involvement, favorable prognosis	-	+ (1/2)	-	-	Mehra, et al. 2013 [3]
Th/To	POP1	lSSc	PF, renal crisis, poor prognosis, myositis, PAH	+ (1/2)	+ (1/1)	+ (3/3)	-	Graf, et al. 2012 [1]; Mehra, et al. 2013 [3]

Table 2 SSc-associated autoantibodies observed in this study *(Continued)*

PL-12	AARS	SSc, PM/DM	ILD without myositis	-	-	+ (1/1)	+ (1/1)	Hamaguchi, et al. 2013 [19]
OJ	IARS	SSc, PM/DM	ILD without myositis	+ (1/1)	-	+ (3/3)	-	Hamaguchi, et al. 2013 [19]
EJ	GARS	SSc, PM/DM	ILD, myositis	-	+ (3/4)	+ (2/2)	+ (0/1)	Hamaguchi, et al. 2013 [19]
Jo-1	HARS	SSc, PM/DM	ILD, myositis	-	+ (1/4)	-	-	Hamaguchi, et al. 2013 [19]
PL-7	TARS	SSc, PM/DM	ILD, myositis	+ (2/2)	++ (8/4)	++ (6/4)	+ (2/4)	Hamaguchi, et al. 2013 [19]
Ha	YARS	SSc, PM/DM	Interstitial pneumonia	-	+ (0/1)	-	-	Hashish, et al 2005 [41]
Zo	**FARSA**, FARSB	SSc, PM/Scl	Anti-synthetase syndrome	-	+ (2/4)	-	-	Betteridge, et al. 2007 [42]
SSc autoantibodies not detected in our dataset								
Fibrillarin	U3RNP	dSSc	More frequent in blacks; severe disease, poor prognosis	-	-	-	-	Mehra, et al. 2013 [3]
U11/U12 RNP	SNRNP35	SSc	Lung fibrosis, gastrointestinal involvement	-	-	-	-	Mimori, 1999 [43]
PDGFR	PDGFR	SSc	Unknown	-	-	-	-	Svegliati Baroni, et al. 2006 [44]
MMP	MMP family	dSSc	Skin, lung, and vascular fibrosis	-	-	-	-	Mehra, et al. 2013 [3]
tPA	PLAT	lSSc	PAH	-	-	-	-	Mehra, et al. 2013 [3]
IFI16	IFI16	lSSc	Common in SARDs	-	-	-	-	Mehra, et al. 2013 [3]
Fibrillin 1	FBN1	dSSc	Choctaw and Japanese patients; absent in Caucasians	-	-	-	-	Mehra, et al. 2013 [3]
Vascular Receptors	AGTR2, EDN1	SSc	TOP1+ patients, renal crisis	-	-	-	-	Mehra, et al. 2013 [3]
ATF2	ATF2	SSc	Longer disease duration, decreased lung function	-	-	-	-	Mehra, et al. 2013 [3]

Data are presented as the average of all peptide hits across each autoantibody group, followed by the frequency of peptide detection within the group. For autoantibodies known to target more than one protein or subunit, data for a single representative protein are shown, with the specific protein highlighted in bold. Associated proteins indicate specific protein targets identified in this study; among autoantibodies not identified here, the most common targets are listed. Symbols: -, +, ++, and +++ indicate an average of 0, 1–4, 5–9, and ≥10 peptide hits per group, respectively

SSc systemic sclerosis, *lSSc* limited cutaneous SSc, *dSSc* diffuse cutaneous SSc, *PAH* pulmonary arterial hypertension; *ILD* interstitial lung disease; *CREST* CREST syndrome (calcinosis, Raynaud phenomenon, esophageal dysmotility, sclerodactyly, and telangiectasia); *PM/Scl* polymyositis/scleroderma, *PM/DM* polymyositis/dermatomyositis

helicases proteins, while community 8 contains a diverse array of proteins including multiple SSc autoantibodies, including TOP1, SSB, Pm/Scl proteins, URNPs, and HNRNPs, and numerous serine/arginine-rich splicing factors. Community 3 consists primarily of aminoacyl tRNA synthetases, a cluster often targeted in autoimmune diseases [19, 23]. Communities 4, 5, and 9 are strongly associated with a variety of GO processes known to play a major role in SSc, including wound healing, IFN signaling, and response to oxidative stress. Major proteins include CD44, HLAs, myosins, and filamin proteins in community 4 and tricarboxylic acid cycle proteins in community 5. Community 9 contains multiple protein disulfide isomerases and peroxiredoxins, protein folding enzymes such as calnexin (CANX) and calreticulin (CALR), and the major collagen processing enzyme prolyl 4-hydroxylase beta (P4HB). Community 6 contains multiple annexin and 14-3-3 proteins; enriched GO processes include ribonucleoprotein complex assembly, mitochondrial transport, RNA processing, and anchoring junction. Community 7 associated with GO terms include cell cycle, RNA polymerase III complex, DNA-PK-Ku complex, and antigen processing and presentation. Community 7 includes several SSc autoantibody targets including Ku proteins XRCC5 and 6, RUVBL1 and 2, RNA polymerase I and II subunits, multiple proteasomal subunits, and T-complex proteins.

Preferential detection of autoantibodies in SSc

Subsequent comparisons between groups were performed in a semiquantitative manner based on the presence or absence of a given protein in an immunoprecipitant, with quantitative analyses limited to comparisons within an individual sample. To identify biological processes and cellular components differentially targeted in SSc, with minimal to no background detection in controls, we examined all proteins detected in >50 % of SSc samples at a frequency >1.5-fold relative to controls, resulting in a list of 137 differentially detected proteins (Fig. 2; Additional file 2: Table S2). Enriched biological processes included *ncRNA metabolic process*, response to oxygen radical, and triglyceride-rich lipoprotein particle remodeling. Preferentially targeted cellular components include cytosolic stress granule, lipid-protein complex, pigment granule, and anchoring junction; molecular functions include antioxidant activity and mRNA binding (Additional file 3: Table S3C).

RNA processing centers are major targets of SSc autoantibodies

The strong enrichment for GO terms associated with mRNA processing and stress response, as well as the identification of cytosolic stress granule as an enriched cellular component, led us to further investigate the role of stress granules (SG) and RNA processing bodies (PB) in the autoantibody response of SSc. SG and PB represent distinct, non-membranous cytoplasmic entities, which arise in response to different cellular stresses including oxidative stress, hypoxia, viral infection, unfolded proteins, and amino acid deprivation [24]. These structures exist in constant flux, driven by the availability of constituent mRNPs, regulating the fate of untranslated mRNAs in response to translational arrest [25]. While SG are generally absent under normal conditions, PB are constitutively present at low levels due to their role as microRNA processing centers. Both structures have been shown to arise in response to cellular stresses, including oxidative stress, ischemia, and cancer [26], all of which are known to be important in SSc pathogenesis [5, 27].

In addition to the 137 differentially detected proteins described above, a wide range of PB/SG constituents were readily detected across most SSc samples (Additional file 5: Table S4). Substantial reactivity was seen against PB components such as UPF1 and MOV10, and SG proteins FXR1 and FXR2, G3BP1 and G3BP2, and USP10. Only background levels of reactivity were seen in healthy controls.

Validation of PB/SG antibodies in SSc

In order to validate the differential abundance of PB/SG proteins identified by LC-MS/MS, HeLa whole cell lysates were immunoprecipitated using antibodies from each patient as described in the LC-MS/MS analyses. Western blots were performed by resolving equal volumes of IP eluates by SDS-PAGE and transferring to nitrocellulose. Blots were then probed with antibodies targeting PB/SG proteins UPF1, MOV10, CAPRIN1, G3BP1, and USP10. These targets were chosen based upon their high level of detection across SSc groups, as determined based on our LC-MS/MS data. Strong reactivity was seen against all five proteins in SSc with only trace levels detected in controls (Fig. 3a), indicating widespread immune responses against these protein complexes.

Further validation was performed using immunofluorescence (IF) staining of U2OS cells maintained under conditions of oxidative stress to induce PB/SG formation. Cells were probed with patient sera in combination with PB and SG markers SK1-Hedls and eIF3b, respectively. Co-localization between patient sera and PB/SG markers was observed in six of nine SSc patients, with at least one positive sample in each of the three autoantibody groups; no staining was seen for any of the three healthy controls (Fig. 3b). These results are consistent with that seen on LC-MS/MS, particularly among RNAP3 patients, who exhibited the strongest and most consistent autoantibody responses across both methods. Taken together, these data strongly implicate PB/SG as novel targets of SSc autoantibody responses.

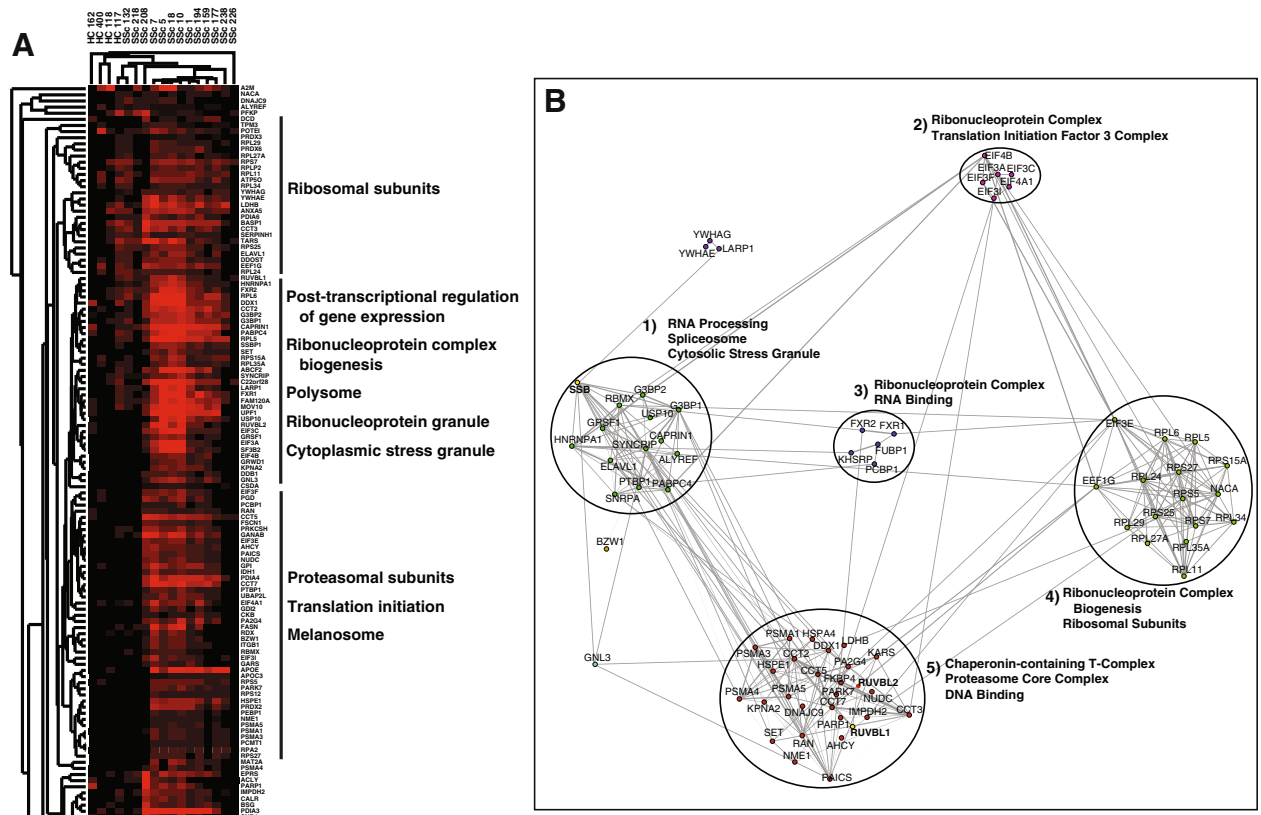

Fig. 2 Proteins differentially detected in systemic sclerosis (*SSc*). Semiquantitative enrichment of SSc-associated autoantibodies was determined using a binary assessment of autoantibody presence or absence in a sample. Preferential enrichment in SSc was defined as all proteins detected in >50 % of all patient samples at a frequency >1.5-fold relative to controls. **a** Heat map of proteins differentially detected in SSc. **b** Network analysis of differentially detected proteins. Community detection was performed using the GIANT global network; functional annotation was performed using gProfiler

Discussion

Autoantibodies have long been used in the diagnosis of SSc, with different autoantibodies predictive of clinical outcomes, including interstitial lung disease, pulmonary arterial hypertension, and skin involvement. While a wide array of SSc-associated autoantibodies have been described, diagnoses are often performed based upon the presence or absence of reactivity against three proteins: RNAP3, TOP1, and CENP. The data presented here suggest a much broader autoantibody response, which is reflective of underlying disease pathologies. Strong subset-specific reactivity was evident against both RNAP3 and TOP1, with no RNAP3 peptides detected in any of the other groups; however, all four RNAP3 patients exhibited modest reactivity against TOP1, indicating a degree of overlap between these two autoantibody groups. When peptides recovered are extended beyond the three major targets, we found substantial overlap across the three major SSc groups. We found peptides from the autoantigens of RuvBL1/2, which appear to act as general markers of SSc, with consistent detection across all SSc groups, with almost no reactivity seen in controls. In contrast, some common SSc autoantigens such as B23 and Ro52/TRIM21 were recovered in virtually all samples, and in controls, indicating an important degree of baseline reactivity against some of the more common autoantibody targets.

In this proof-of-concept study, we do not attempt to address the clinical implications of the autoantibody responses described here due to the limited number of patients analyzed, nor are we able to speculate on the presence or absence of these autoantibodies in other SSc autoantibody groups. Our depth in this study comes from the number of potential antigens analyzed, which cover the full proteome. Future studies examining a much larger cohort of SSc patients, along with representatives of other

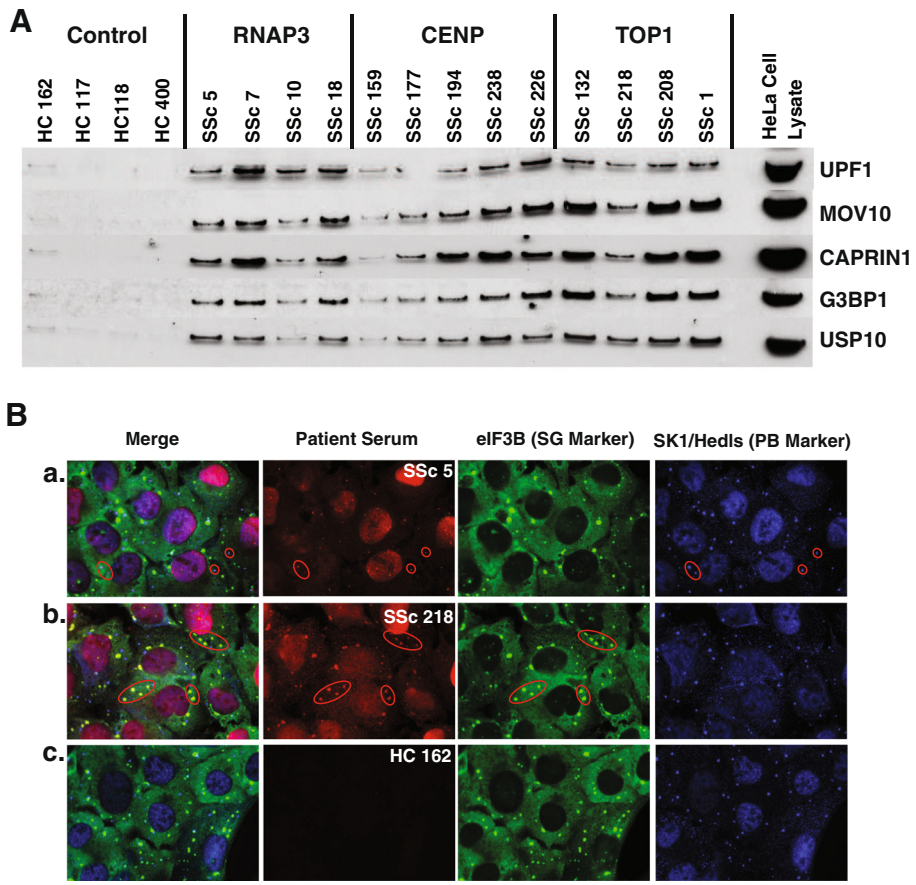

Fig. 3 Validation of RNA processing bodies (*PB*)/stress granules (*SG*) as a target of the SSc autoimmune response. **a** HeLa cell lysates were immunoprecipitated using patient sera, resolved by SDS-PAGE, and probed with antibodies targeting known PB and SG proteins; HeLa whole cell lysate was used as a control. **b** Immunofluorescence was performed in U2OS cells treated with sodium (meta)arsenite to induce the formation of SG. Cells were then fixed with 4 % paraformaldehyde and permeabilized with 5 % normal horse serum and 0.1 % digitonin in Tris-buffered saline. Staining was performed with anti-eIF3b (SG marker), anti-SK1-Hedls (PB marker), and patient sera. Representative images depicting co-localization between patient sera and SG/PB markers are shown, with sites of co-localization circled in *red*. *RNAP* RNA polymerase, *CENP* centromere protein *TOPI* topoisomerase I

autoimmune diseases, will be necessary to determine the clinical value of these potential autoantibodies.

This is not the first study to suggest the presence of multiple autoantibodies in SSc. Immunoassays performed by Op De Beeck, et al. revealed the presence of multiple autoantibodies in a small subset of SSc patients [28]. A similar analysis by Graf et al. using the EUROLINE immunoassay revealed the presence of multiple autoantibodies in 11 % of patients [1].

Autoantibodies against extracellular immune signaling receptors and extracellular matrix proteins were conspicuously absent in these data; this includes the absence of numerous autoantibodies previously implicated in SSc pathogenesis, such as anti-fibrillin 1, anti-MMP, and anti-PDGFR [29]. Additional analyses in other cell types, such as fibroblasts or endothelial cells, and cells maintained under physiologically relevant growth conditions, such as immune activation or oxidative stress, may be useful for identifying other proteins and complexes which may play a role in disease pathogenesis.

In addition to identifying novel autoantibody targets, the unbiased nature of mass spectrometry provides additional insights into the processes potentially underlying autoimmunity. The preferential detection of proteins associated with RNA processing and oxidative stress as a general feature of SSc autoantibodies may be indicative of their origins. Combined with the consistent targeting of PB/SG described here spanning all SSc patients, these data suggest a basic model in which disease-specific pathologies give rise to specific autoantibodies. Strong induction of SGs is observed in response to cellular stresses, including oxidative stress and ischemia, two well-established phenomena in SSc [27]. SG/PB are also readily induced in response to the tumor microenvironment, consistent with recent evidence linking RNAP3-positive SSc and cancer [5, 30]. Combined with evidence

linking transforming growth factor (TGF)-β signaling with an increase in PB formation [31], many of the major processes underlying SSc pathogenesis appear broadly consistent with an immune response against cells undergoing a stress response. PBs are also known to associate with other cytoplasmic structures, such as U bodies [32], which house an number of well-established SSc autoantibody targets, including U1, U5, and U11/U12. Taken together, these data suggest a model in which autoantibodies arise as a secondary phenotype in response to SSc-related processes already underway.

Some evidence suggesting a link between PBs and autoimmunity has been described previously. Bhanji, et al. observed reactivity against a number of PB-associated proteins, including GE1/*Hedls*, GW182, and Ago2 in a range of autoimmune diseases, including SSc [33]. Among these autoantigens, only Ago2 was also identified in this analysis, suggesting a persistent, yet diverse response against this complex. A similar analysis of SG-associated proteins has not been performed; however given the reactivity to PB proteins seen in other autoimmune diseases, reactivity in other autoimmune diseases is possible. A detailed analysis using both mass spectrometry and other methods will be necessary to understand the degree to which autoantibodies to SG/PBs are seen in other autoimmune diseases, and the clinical implications of these findings.

This work has several limitations. First, we cannot eliminate the possibility that some proteins found in our mass spectrometry data result from co-IP of multiprotein complexes by a single autoantibody; however, we were able to confirm the presence of multiple PB/SG autoantibodies by other means (Fig. 3). We also cannot rule out the possibility that some targets were missed due to their being sequestered into tightly packed molecular complexes associated with chromatin. For example, the presence of CENP autoantibodies within these samples had been established using clinical methods, indicating its absence in our mass spectrometry data is likely a result of its sequestration into large macromolecular complexes with limited solubility. A lack of age- and gender-matched controls likely underestimates the degree of baseline reactivity seen in unaffected controls. Finally, the small number of patient samples used in this study prevents any clinical interpretation, and the variability in the number of peptides recovered between experiments limits direct quantitative comparisons between autoantibody groups.

Conclusions

The data presented here provide evidence of diverse immune reactivities in SSc targeting a wide array of protein complexes. Among these complexes, autoantibodies targeting PB/SG were consistently identified across both clinical SSc subsets and major autoantibody groups, suggesting a potential novel autoantibody target. Taken together, these data suggest immune responses to proteins involved in cellular stress may be a common mechanism for autoantibody generation.

Additional files

Additional file 1: Table S1. Complete list of peptides identified in this analysis. *TP* number of total peptides mapping to a protein, *UP* number of unique peptides mapping to a protein, *UM* number of non-redundant peptides mapping exclusively to a protein, *MW* molecular weight, *Length* protein length in amino acids. (XLS 639 kb)

Additional file 2: Table S2. Gene lists used in these analyses. (XLSX 17 kb)

Additional file 3: Table S3. Systemic sclerosis (SSc)-specific enrichment of processes and components. Proteins differentially detected in SSc were analyzed using gProfiler. Statistically significant processes and components are shown. A) Peptides detected at any level across all four groups. B) Peptides identified in all SSc groups, but absent in controls. C) Analysis of 137 proteins differentially detected in SSc. *BP* biological process, *CC* cellular component, *MF* molecular function, *ke* KEGG pathway, *re* REACTOME pathway. (ODS 70 kb)

Additional file 4: Figure S1. Network analysis of systemic sclerosis (SSc) autoantigens. All 763 non-redundant peptide hits identified in two or more patients were analyzed using the Genome-scale Integrated Analysis of gene Networks in Tissues (GIANT) global network to identify functionally associated protein networks. Analysis of community function was performed using gProfiler. SSc-associated autoantibodies are highlighted in *yellow*. (EPS 1902 kb)

Additional file 5: Table S4. Processing body and stress granule proteins identified in this analysis. *Proteins with multiple subunits. Data indicate non-redundant peptide hits. (ODS 20 kb)

Abbreviations

CENP: centromere protein; DMEM: Dulbecco's modified Eagle's medium; dSSc: diffuse systemic sclerosis; ELISA: enzyme-linked immunosorbent assay; FBS: fetal bovine serum; GIANT: Genome-scale Integrated Analysis of gene Networks in Tissues; IFN: interferon; kDa: kiloDalton; LC-MS/MS: liquid chromatography tandem-mass spectrometry; IP: immunoprecipitation; lSSc: limited systemic sclerosis; PB: RNA processing bodies; PBS: phosphate-buffered saline; RNAP3: RNA polymerase III; SG: stress granules; SSc: systemic sclerosis; TOP1: topoisomerase I.

Competing interests

Dr. Whitfield has received royalties for patents regarding gene expression biomarkers in Scleroderma and is a scientific founder of Celdara Medical LLC. Dr. Lafyatis has received both grants and consulting fees from Genzyme/Sanofi, Shire, Regeneron, Biogen, BMS, Inception, Precision Dermatology, PRISM, UCB, Pfizer and Roche/Genentech; he received consulting fees from Lycera, Novartis, Celgene, Amira, Celdara, Celltex, Dart Therapeutics, Idera, Intermune, Medimmune, Promedior, Zwitter, Actelion, EMD Serono, Akros, Extera, Reneo, Scholar Rock, and HGS. No authors have any non-financial conflicts of interest to report.

Authors' contributions

MEJ conceived of the study, performed experiments, analyzed data, and wrote the manuscript. AVG performed mass spectrometry and helped to revise the manuscript. JNT performed data analysis and helped to revise the manuscript. SML performed immunofluorescence experiments, and helped to revise the manuscript. DS performed mass spectrometry, and revised the manuscript. JKG, RFS, and RL provided clinical samples, and revised the manuscript. PJA designed experiments, provided technical assistance, and revised the manuscript. SAG and MLW conceived of the study, participated in its design, and helped to revise the manuscript. All authors read and approved the final manuscript.

Acknowledgements
This work was supported by grants from the NIH National Institute of Arthritis and Musculoskeletal and Skin Diseases (NIAMS) Center of Research Translation (P50 AR060780 to MLW and RL), the Department of Defense (PR130908 to MLW), and a SYNERGY grant from the Geisel School of Medicine at Dartmouth (to MLW). JNT is supported in part by a grant from the National Institute of General Medical Sciences (NIGMS; T32GM008704). SAG is supported by grants R01-CA155260 and S10-OD016212 from the NIH. JKG is supported by a Kellen Foundation Clinician Scientist Development Award from the Hospital for Special Surgery. Written informed consent was obtained from all participants for publication of their individual details in this manuscript. All consent forms are held by the respective authors' institutions and are available for review by the Editor-in-Chief.

Author details
[1]Department of Genetics, Geisel School of Medicine at Dartmouth, Hanover, NH, USA. [2]Division of Rheumatology, Immunology, and Allergy, Brigham and Women's Hospital, Boston, MA, USA. [3]Department of Rheumatology, Hospital for Special Surgery, New York, NY, USA. [4]Boston University School of Medicine, Boston, MA, USA. [5]Dartmouth Medical School, Hinman Box 7400, Hanover, NH 03755, USA.

Received: 6 October 2015 Accepted: 3 January 2016
Published online: 22 January 2016

References

1. Graf SW, Hakendorf P, Lester S, Patterson K, Walker JG, Smith MD, et al. South Australian Scleroderma Register: autoantibodies as predictive biomarkers of phenotype and outcome. Int J Rheum Dis. 2012;15:102–9.
2. Steen VD. Autoantibodies in systemic sclerosis. Semin Arthritis Rheum. 2005; 35:35–42.
3. Mehra S, Walker J, Patterson K, Fritzler MJ. Autoantibodies in systemic sclerosis. Autoimmun Rev. 2013;12:340–54.
4. Fertig N, Domsic RT, Rodriguez-Reyna T, Kuwana M, Lucas M, Medsger TA, et al. Anti–U11/U12 RNP antibodies in systemic sclerosis: A new serologic marker associated with pulmonary fibrosis. Arthritis Care Res. 2009;61:958–65.
5. Joseph CG, Darrah E, Shah AA, Skora AD, Casciola-Rosen LA, Wigley FM, et al. Association of the autoimmune disease scleroderma with an immunologic response to cancer. Science. 2014;343:152–7.
6. Robinson WH, DiGennaro C, Hueber W, Haab BB, Kamachi M, Dean EJ, et al. Autoantigen microarrays for multiplex characterization of autoantibody responses. Nat Med. 2002;8:295–301.
7. Yore MM, Kettenbach AN, Sporn MB, Gerber SA, Liby KT. Proteomic analysis shows synthetic oleanane triterpenoid binds to mTOR. PLoS ONE. 2011;6:e22862.
8. Eng JK, Jahan TA, Hoopmann MR. Comet: An open-source MS/MS sequence database search tool. Proteomics. 2013;13:22–4.
9. Hsieh EJ, Hoopmann MR, MacLean B, MacCoss MJ. Comparison of database search strategies for high precursor mass accuracy MS/MS data. J Proteome Res. 2009;9:1138–43.
10. Elias JE, Gygi SP. Target-decoy search strategy for increased confidence in large-scale protein identifications by mass spectrometry. Nat Methods. 2007;4:207–14.
11. Oliveros JC. VENNY. An interactive tool for comparing lists with Venn Diagrams. 2007.
12. Greene CS, Krishnan A, Wong AK, Ricciotti E, Zelaya RA, Himmelstein DS, et al. Zaslavsky E. Understanding multicellular function and disease with human tissue-specific networks. Nat Genet. 2015;47:569–76.
13. Shannon P, Markiel A, Ozier O, Baliga NS, Wang JT, Ramage D, et al. Cytoscape: a software environment for integrated models of biomolecular interaction networks. Genome Res. 2003;13:2498–504.
14. Reimand J, Arak T, Vilo J. g: Profiler—a web server for functional interpretation of gene lists (2011 update). Nucleic Acids Res. 2011;39:W307–15.
15. Eisen MB, Spellman PT, Brown PO, Botstein D. Cluster analysis and display of genome-wide expression patterns. PNAS. 1998;95:14863–8.
16. Saldanha AJ. Java Treeview—extensible visualization of microarray data. Bioinformatics. 2004;20:3246–8.
17. Novoradovskaya N, Perou C, Whitfield M, Basehore S, Pesich R, Aprelikova O, et al.: Universal human, mouse and rat reference RNA as standards for microarray experiments. In: Mol Bio Cell: 2002: Amer Soc Cell Biology 8120 Woodmont Ave, STE 750, Bethesda, MD 20814-2755 USA; 2002: 241A-241A.
18. Kaji K, Fertig N, Medsger TA, Satoh T, Hoshino K, Hamaguchi Y, et al. Autoantibodies to RuvBL1 and RuvBL2: A novel systemic sclerosis-related antibody associated with diffuse cutaneous and skeletal muscle involvement. Arthr Care Res. 2014;66:575–84.
19. Hamaguchi Y, Fujimoto M, Matsushita T, Kaji K, Komura K, Hasegawa M, et al. Common and Distinct Clinical Features in Adult Patients with Anti-Aminoacyl-tRNA Synthetase Antibodies: Heterogeneity within the Syndrome. PLoS ONE. 2013;8:e60442.
20. Fujimoto M, Shimozuma M, Yazawa N, Kubo M, Ihn H, Sato S, et al. Prevalence and clinical relevance of 52-kDa and 60-kDa Ro/SS-A autoantibodies in Japanese patients with systemic sclerosis. Ann Rheum Dis. 1997;56:667–70.
21. Ulanet DB, Wigley FM, Gelber AC, Rosen A. Autoantibodies against B23, a nucleolar phosphoprotein, occur in scleroderma and are associated with pulmonary hypertension. Arth Care Res. 2003;49:85–92.
22. Brouwer R, Vree Egberts WTM, Hengstman GJD, Raijmakers R, van Engelen BGM, Peter Seelig H, et al. Autoantibodies directed to novel components of the PM/Scl complex, the human exosome. Arth Res. 2002;4:134–8.
23. Lega J-C, Fabien N, Reynaud Q, Durieu I, Durupt S, Dutertre M, et al. The clinical phenotype associated with myositis-specific and associated autoantibodies: A meta-analysis revisiting the so-called antisynthetase syndrome. Autoimmun Rev. 2014;13:883–91.
24. Kedersha N, Ivanov P, Anderson P. Stress granules and cell signaling: more than just a passing phase? Trends Biochem Sci. 2013;38:494–506.
25. Kedersha N, Anderson P. Regulation of translation by stress granules and processing bodies. Prog Mol Biol Transl Sci. 2009;90:155–185.
26. Anderson P, Kedersha N. Stress granules: the Tao of RNA triage. Trends Biochem Sci. 2008;33:141–50.
27. Katsumoto TR, Whitfield ML, Connolly MK. The pathogenesis of systemic sclerosis. Annu Rev Pathol-Mech. 2011;6:509–37.
28. Op De Beéck K, Vermeersch P, Verschueren P, Westhovens R, Mariën G, Blockmans D, et al. Antinuclear antibody detection by automated multiplex immunoassay in untreated patients at the time of diagnosis. Autoimmun Rev. 2012;12:137–43.
29. Chung L, Utz P. Antibodies in scleroderma: Direct pathogenicity and phenotypic associations. Curr Rheumatol Rep. 2004;6:156–63.
30. Anderson P, Kedersha N, Ivanov P. Stress granules, P-bodies and cancer. Biochim Biophys Acta. 2015, 1849, 861–870.
31. Blanco FF, Sanduja S, Deane NG, Blackshear PJ, Dixon DA. Transforming growth factor β regulates P-body formation through induction of the mRNA decay factor tristetraprolin. Mol Cell Bio. 2014;34:180–95.
32. Liu J-L, Gall JG. U bodies are cytoplasmic structures that contain uridine-rich small nuclear ribonucleoproteins and associate with P bodies. PNAS. 2007; 104:11655–9.
33. Bhanji RA, Eystathioy T, Chan EKL, Bloch DB, Fritzler MJ. Clinical and serological features of patients with autoantibodies to GW/P bodies. Clin Immunol. 2007;125:247–56.
34. Dib H, Tamby MC, Bussone G, Regent A, Berezné A, Lafine C, Broussard C, Simonneau G, Guillevin L, Witko-Sarsat V, et al. Targets of anti-endothelial cell antibodies in pulmonary hypertension and scleroderma. Eur Respir J. 2012;39(6):1405–1414.
35. Naniwa T, Sugiura Y, Banno S, Yoshinouchi T, Matsumoto Y, Ueda R. Ribosomal P protein P0 as a candidate for the target antigen of anti-endothelial cell antibodies in mixed connective tissue. Clin Exp Rheumatol. 2007;25:593–598.
36. Terrier B, Tamby MC, Camoin L, Guilpain P, Broussard C, Bussone G, et al. Identification of target antigens of antifibroblast antibodies in pulmonary arterial hypertension. Am J Resp Crit Care Med. 2008;177(10):1128–1134.
37. Terrier B, Tamby MC, Camoin L, Guilpain P, Bérézné A, Tamas N, et al. Anti-fibroblast antibodies from systemic sclerosis patients bind to α-enolase and are associated with interstitial lung disease. Ann Rheum Dis. 2009.
38. Satoh M, Chan JY, Ceribelli A, del-Mercado MV, Chan EK. Autoantibodies to Argonaute 2 (Su antigen). In: Ten Years of Progress in GW/P Body Research. Springer. 2013:45-59.
39. Siapka S, Patrinou-Georgoula M, Vlachoyiannopoulos PG, Guialis A. Multiple specificities of autoantibodies against hnRNP A/B proteins in systemic rheumatic diseases and hnRNP L as an associated novel autoantigen. Autoimmunity. 2007;40(3):223–233.
40. Kubo M, Ihn H, Kuwana M, Asano Y, Tamaki T, Yamane K, Tamaki K. Anti-U5 snRNP antibody as a possible serological marker for scleroderma–polymyositis overlap. Rheumatol. 2002;41(5):531–534.

41. Hashish L, Trieu E, Sadanandan P, Targoff I. Identification of autoantibodies to tyrosyl-tRNA synthetase in dermatomyositis with features consistent with anti-synthetase syndrome. In: Arthritis Rheum. 2005; 2005: S312-S312
42. Betteridge Z, Gunawardena H, North J, Slinn J, McHugh N. Anti-synthetase syndrome: a new autoantibody to phenylalanyl transfer RNA synthetase (anti-Zo) associated with polymyositis and interstitial pneumonia. Rheumatol. 2007;46(6):1005–1008.
43. Mimori T. Autoantibodies in Connective Tissue Diseases. Clinical Significance and Analysis of Target Autoantigens. Internal Med. 1999;38(7):523–532.
44. Svegliati BS, Santillo M, Bevilacqua F, Luchetti M, Spadoni T, Mancini M, et al. Stimulatory autoantibodies to the PDGF receptor in systemic sclerosis. N Engl J Med. 2006;354(25):2667–2676.